Kaunas University of Technology

Mathematics and Natural Sciences

Evaluation of Head and Neck Cancer Irradiation with a High Energy Photons Using Individualized 3D Printed Bolus

Master's Final Degree Project

Lali Keshelava

Project author

Lect. Dr. Jurgita Laurikaitiene

Supervisor

Kaunas, 2020.

Kaunas University of Technology

Mathematics and Natural Sciences

Evaluation of Head and Neck Cancer Irradiation with a High Energy Photons Using Individualized 3D Printed Bolus

Master's Final Degree Project

Medical Physics (**6213GX001**)

Lali Keshelava

Project author

Lect. Dr. Jurgita Laurikaitiene

Supervisor

Prof. Giedrius Laukaitis

Reviewer

Kaunas, 2020.

Kaunas University of Technology

Mathematics and Natural Sciences

Lali Keshelava

Evaluation of Head and Neck Cancer Irradiation with a High Energy Photons Using Individualized 3D Printed Bolus

Declaration of Academic Integrity

I confirm that the final project of mine, Lali Keshelava, on the topic „Evaluation of Head and Neck Cancer Irradiation with a High Energy Photons Using Individualized 3D Printed Bolus“ is written completely by myself; all the provided data and research results are correct and have been obtained honestly. None of the parts of this thesis have been plagiarised from any printed, Internet-based or otherwise recorded sources. All direct and indirect quotations from external resources are indicated in the list of references. No monetary funds (unless required by Law) have been paid to anyone for any contribution to this project.

I fully and completely understand that any discovery of any manifestations/case/facts of dishonesty inevitably results in me incurring a penalty according to the procedure(s) effective at Kaunas University of Technology.

Lali Keshelava — (name and surname filled in by hand)

L. Keshelava — (signature)

Lali Keshelava. Evaluation of Head and Neck Cancer Irradiation with a High Energy Photons Using Individualized 3D Printed Bolus. Master's Final Degree Project / supervisor Lect. Dr., Jurgita Laurikaitiene; Mathematics and Natural Sciences, Kaunas University of Technology.

Study field and area (study field group): Health Sciences (Medical Technology).

Keywords: bolus, 3D Printing, Head and Neck shallow tumors, 3D printed boluses, 3D Treatment planning

Kaunas, 2020. 62.

Summary

The bolus is the build-up human tissue-equivalent material placed directly on the patient's surface. Build-up bolus creates a dose build-up during irradiation using a high-energy (MeV) photons beam. The main problem using bolus is formed air gaps, between the bolus and a patient's surface, which affects an isodose distribution on the skin/ surface. To avoid air gaps three-dimensional printing technique could be used creating bolus individually for each patient, recreating it from the real patient’s computed tomography (CT) images.

In this research project two different thickness (0.5 cm and 1.0 cm) individualized 3D printed polylactic acid (PLA) boluses were used for the head and neck (eyes and nose region) cancer irradiation imitation. For this reason was created patient-specific phantom based on the patient‘s CT scans and the head CT polymethyl methacrylate (PMMA) phantom. Patient-specific phantom CT scans were used for two different thickness (0.5 cm and 1.0 cm) individualized 3D printed boluses fabrication.

Evaluation of the formed air gaps was done using the 3D treatment planning system “Eclipse“, which showed that the air gaps formed under 0.5 cm and 1.0 cm individualized 3D printed bolus was almost symmetrical. For 0.5 cm thickness bolus the air gaps varied from 0.4 mm to 2.1 mm, while for 1.0 cm thickness bolus it varied from 0.6 mm to 2.2 mm (the cheeks area), meanwhile on the nose region for 0.5 cm thickness bolus varied from 0.7 mm to 1.3 mm, for 1.0 cm thickness – 1.4 mm maximum air gap was observed.

A single field plans isodose distribution and surface volume coverage were analyzed without bolus and with 0.5 cm thickness and 1.0 cm thickness boluses. The results were compared to the 2 Gy prescribed dose, which showed that 95 %, 98 % and 99 % of surface volume coverage for a single field plan with 0.5 cm thickness bolus were 0.5 %, 2.0 % and 3.0 % respectively, while for 1.0 cm thickness – 0.0 % (for 95 %), 0.5 % (for 98 %) and 1.5 % (for 99 %). The most significant difference was observed for the single field plan without bolus, which showed more than 40.0 % for the 95 % surface volume coverage, 50.0 % (for 98 %), and 52.0 % (for 99 %).

The research work showed that individualized 3D printed bolus could be reliable and may improve the shallow tumor irradiation treatment outcome.

Lali Keshelave. Galvos ir kaklo apšvitos didelės energijos fotonais vertinimas panaudojant individualizuotą 3D spausdintuvu atspausdintą bolusą. Magistro baigiamasis projektas / vadovas dr. Jurgita Laurikaitienė; Kauno technologijos universitetas, Matematikos ir gamtos mokslų fakultetas.

Mokslo kryptis ir sritis: Sveikatos mokslai (Medicinos technologijos)i

Reikšminiai žodžiai: *bolusas, 3D spausdinimas, galvos ir kaklo paviršiniai navikai, 3D gydymo planavimo sistema*

Kaunas, 2020. 62 p.

Santrauka

Bolusas yra kaip papildoma žmogaus audiniui lygiavertė medžiaga dedama tiesiogiai ant paciento. Bolusas sukuria dozės „kaupimo“ sritį apšvitos metu naudojant didelės energijos (MeV) fotonų pluoštą. Pagrindinė problema naudojant bolusą yra susidarantys oro tarpai tarp boluso ir paciento paviršiaus, kurie turi įtakos izodozių pasiskirstymui ant odos/ paviršiaus. Norint išvengti oro tarpų trimatė spausdinimo technologija gali būti naudojama sukuriant bolusą individualiai kiekvienam pacientui, atkuriant bolusą iš paciento kompiuterinės tomografijos (KT) vaizdų.

Šiame projektiniame baigiamajame darbe buvo atspausdinti du skirtingo storio (0,5 cm ir 1,0 cm) individualizuoti 3D polilaktinės rūgšties (PR) bolusai galvos ir kaklo (akių ir nosies sritis) vėžio apšvitos procedūrai imituoti/ simuliuoti. Dėl šios priežasties buvo sukurtas pacientą atkartojantis (imituojantis) fantomas panaudojant paciento KT skenus ir galvos KT polimetil meta akrilato (PMMA) fantomą. KT nuskenuotas pacientą atkartojantis (imituojantis) fantomas buvo panaudotas atkuriant du skirtingo storio (0,5 cm ir 1,0 cm) individualizuotus 3D spausdintuvu atspausdintus bolusus.

Susidariusių oro tarpų tyrimas buvo atliktas naudojantis 3D gydymo planavimo sistema „Eclipse“. Oro tarpai po 0,5 cm ir 1,0 cm individualizuoto 3D spausdintuvu atspausdinto boluso susiformavo simetriškai. Oro tarpai susiformavę skruostų srityje po 0,5 cm storio bolusu kito nuo 0,4 mm to 2,1 mm, o po 1,0 cm storio bolusu kito nuo 0,6 mm to 2,2 mm, kai tuo tarpu nosies srityje po 0,5 cm storio bolusu oro tarpai kito nuo 0,7 mm iki 1,3 mm; po 1 cm storio bolusu buvo suformuotas tik 1,4 mm maksimalus oro tarpas.

Izodozių pasiskirstymas bei paviršiaus tūrio apšvita buvo analizuojama vieno apšvitos lauko sukurtuose planuose be boluso ir su 0,5 cm bei 1,0 cm storio bolusais. Gauti rezultatai buvo palyginti su 2 Gy paskirtąja doze. Gauta, kad 95 %, 98 % ir 99 % tūrio paviršius su 0,5 cm storio bolusu skyrėsi 0,5 %, 2,0 % ir 3,0 % atitinkamai, kai tuo tarpu 1,0 cm storio – 0,0 % (95 %), 0,5 % (98 %) ir 1,5 % (99 %). Didžiausias skirtumas buvo stebimas vieno apšvitos lauko plane be boluso, kuris buvo didesnis negu 40,0 % (95 % tūrio paviršiui), 50,0 % (98 %), ir 52,0 % (99 %).

Taigi 3D spausdintuvu atspausdintas bolusas yra patikimas ir gali pagerinti paviršiuje esančių galvos ir kaklo navikų spindulinio gydymo kokybę.

Table of Contents

List of figures

List of tables

List of abbreviations and terms

3D – three dimensional

3D CRT – 3D Conformal Radiathion Therapy

ABS – Acrylonitrile butadiene styrene

AD – Absorbed dose;

CT – Computed tomography;

CPE – Charged particle equilibrium

$D_{surf.}$ – Surface dose;

DICOM – Digital images and communications in medicine;

DLP – Digital light processing

FDM – Fused Deposition Modelling

Gy – Grey

H&N – Head and Neck

HU – Hounsfield units

IMRT – Intesity Modulated Radiation Therapy

MeV – Mega electron volt;

MV – Mega volt

NTCP – Normal tissue complication probability;

OAR – Organs at risk

OD – Optical density

OSL – Optically stimulated luminescence

PDD – Percentage Depth Dose

PLA – Polylactic acid plastic;

PMMA – Poly methyl methacrylate

PTV – Planning Target Volume

PV – Pixel value

QA – Quality assurance

SLS – Selective Laser Sintering

SSD – Source to surface distance;

STL – Stereolithography

TLD – Thermoluminescent dosimeter

TPS – Treatment planning system;

VMAT – Volumetric Arc Radiation Therapy

Introduction

Irradiation of uneven and complex shape geometry of the human body results in inhomogeneity of the dose distribution on the surface. High energy (MeV) photons beam irradiation results in a skin-sparing effect that reduces treatment outcomes during the irradiation of shallow tumors. One of the solutions to use so-called additional body – bolus. Bolus (build-up material) is a human tissue equivalent additional body layer placed on the patient's surface, which results in an increased dose to the surface and minimized the ability for the disease recurrence. One of the challenges using boluses is air gaps formed between bolus and patient surface, which create inhomogeneity of dose distribution and slightly minimized dose on the surface. The larger the air gap, the less the absorbed dose on the patient surface is, for example, 4 mm air gap means approximately 4 % dose reduction, while 10 mm – ~10 %, using standard silicone bolus [1, 2]. Therefore, the *importance* of irradiating uneven or/ and concaved surface and shallow tumors, especially for head and neck cancer irradiation, is to avoid or minimize formed air gaps, so ensuring the better treatment outcome. Due to this reason today as an alternative could be used *modern and new* 3D printing technique, for individualized tissues equivalent patient-specific phantoms (anthropomorphic) and boluses printing, which start to be more often used in a clinical environment. Individualized 3D printed boluses showed really promising results for avoidance and minimization of the formed air gaps (up to 1-2 mm) [1, 2] in between in comparison with a standard silicone bolus (larger than 4 mm) [1]. So the main *problem, relevance, and novelty* of this research project are to ensure better treatment outcomes using and implementing individualized 3D printed PLA bolus in clinical practice, ensuring better disease control irradiating head and neck shallow tumors.

This research work aims to determine and evaluate the suitability of individualized 3D printed polylactic acid (PLA) bolus imitating shallow head and neck cancer irradiation procedure.

The tasks:

1. To reconstruct and print different thickness (0.5 cm and 1.0 cm) individualized 3D printed PLA boluses, for a patient-specific phantom used imitating shallow head and neck cancer irradiation procedure;

2. To analyze the size of the air gaps formed between different thickness (0.5 cm and 1.0 cm) individualized 3D printed PLA boluses and patient-specific phantom;

3. To analyze 3D treatment single field plans without bolus and with individualized 3D printed PLA bolus.

3D printing of boluses and the patient's specific phantom (it was printed by Ph.D. student Antonio Jreije (KTU)) were performed in Kaunas University of Technology, while dosimetric evaluation of the results was done in Oncology Hospital of the Hospital of Lithuanian University of Health Sciences Kaunas Clinics.

1 Literature Review

1.1 The main aspects of the shallow head and neck tumours irradiation using high energy photons

Head and neck (H&N) cancer are one of the most common cancer localization with its complex geometry/ anatomy. The main purpose of radiation therapy is to irradiate tumor and save critical organs as much as possible, but due to H&N anatomy issues sometimes it is hard to avoid unnecessary dose to the healthy tissues or organs at risk (OARs), such as: spinal cord, salivary and parotid glands, thyroid, esophagus which are in the close vicinity of the irradiated tumor, etc. (figure 1) [3-4].

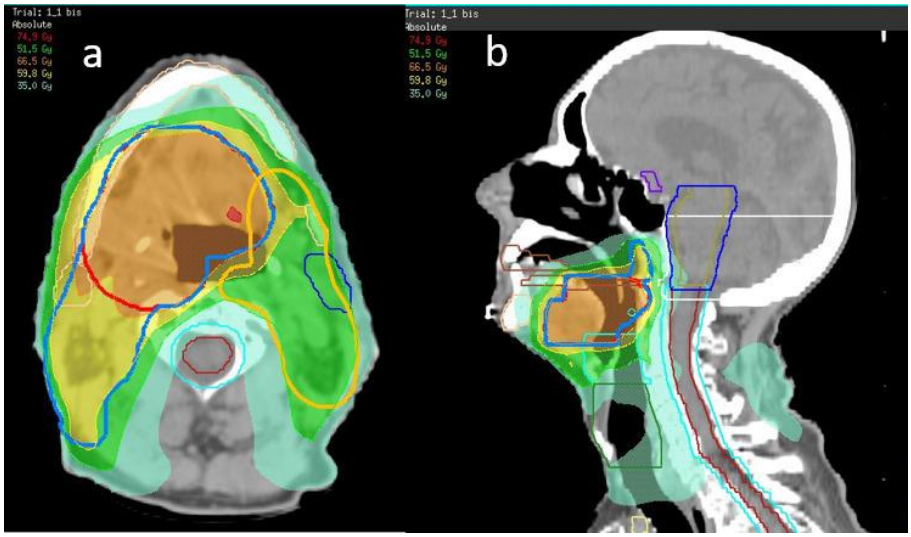

Fig. 1. Intensity Modulated Radiation Therapy (IMRT) plan for oropharyngeal lesions with 5mm isotropic margins tumor volume and OARs in close vicinity. The critical organ in this case in spinal cord (marked as red (a, b)), while the isocenter is oropharingeal lesions (marked as blue filled with orange (Figure 1 b)). IMRT with VMAT (Volumetric Arc Radiation Therapy) is applied in order to protect critical organs, but it could be clearly seen that OARs: trachea (Figure 1 b square), lower jawable mandible and its lymph nodes still recieve percent of prescribed dose [5]

Therefore, due to H&N tumors, which usually are located close to the critical organs, high accuracy is needed for the prescribed dose delivery to the target. So the main task is to find out the most appropriate irradiation technique/ method for the H&N cancer patients' treatment, ensuring the delivery of the maximum prescribed dose, at the same time trying to save healthy tissues and critical organs. There are used two different irradiation treatment planning techniques, using a high energy photon (> 4 MeV), like inverse treatment planning (Intensity-modulated radiotherapy (IMRT), volumetric-modulated arc therapy (VMAT)) and forward treatment planning (3D conformal radiotherapy (3D-CRT)) (figure 2). It is known, that inverse treatment planning is defined as a method of treatment planning, which starts from the desired distribution of the dose or clinical objectives, and just after that there are determined parameters of the

treatment, which allows achieving it. While, the conventional forward treatment planning technique starts from treatment parameters, which first are chosen, and just afterward the dose distribution is calculated and evaluated [6].

A

B

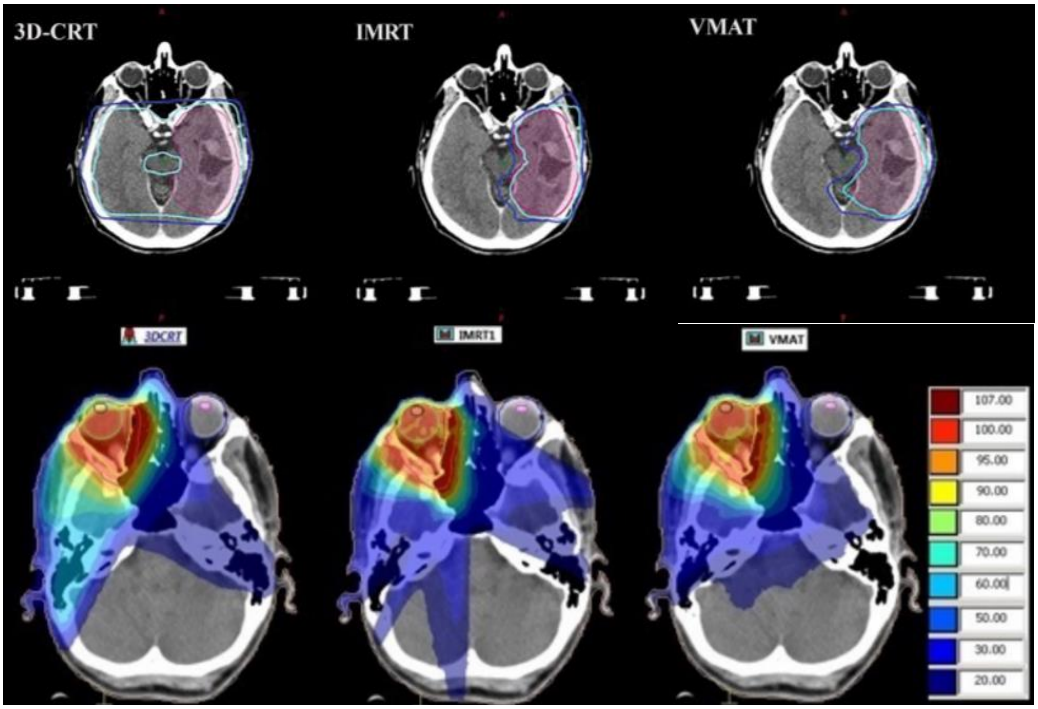

Fig. 2. A - Example of the dose distribution using 3D-CRT, IMRT and VMAT treatment planning techniques for the same brain cancer patient [5], B – Illustration of the dose distribution of 3D-CRT, IMRT, VMAT treatment plan, while the treatment region is eye [7]

Such kinds of technological innovations, like inverse treatment planning fully have changed the way of H&N cancer treatment, especially comparing the doses of OARs with 3D CRT (Table 1) [8]. The results show, that the critical organ doses are significantly higher for brain and esophagus and may increases the probability of such side effects, like brain radionecrosis, esophagitis (inflammation of the esophagus.) or swallowing disorder (dysphagia) for the patient, using 3D CRT technique for H&N cancer patients [5, 8].

Table 1. Doses to organs at risk (OAR) for VMAT, IMRT and 3D-CRT, for H&N cancer (dose per whole treatment is 66 Gy) [8]

OAR	**VMAT**		**IMRT**		**3DCRT**	
	Mean dose (Gy)	**Maximum dose (Gy)**	**Mean dose (Gy)**	**Maximum dose (Gy)**	**Mean dose (Gy)**	**Maximum dose (Gy)**
Esophagus	14	23	17	29	37	40
Brain	21	40	21	42	31	56

H&N cancer patient's irradiation today is usually performed using the VMAT technique, even coverage of tumor and sparing of OARs using IMRT and VMAT techniques are similar (figure 2). The main argument for this is that VMAT is faster, due to this reason it results in a lower probability of the patient movements during the irradiation procedure, so ensuring accuracy and outcome of the treatment procedure. Accuracy of irradiation procedure is a very important aspect irradiating H&N tumors, due to a sharp dose falloff outside the volume of the tumor, why the protection of the OARs, which are in so close vicinity of the tumor is so important and plays the main role [9]. Accuracy of the treatment procedure is closely related to the quality assurance (QA), which is the main prevention of mistakes or quality control (QC), which let us detect possible problems [5]. For example, it is required that the delivery accuracy of the absorbed dose to the target has to be ±5% or in critical situations ±2% [10].

1.2 Dosimetry in external beam radiotherapy

Dosimetry is one of the most important tools in radiotherapy that determines the safe and accurate dose delivery. There are several methods of dose-measuring, correctly reflecting the accuracy of the dose delivery, using complex irradiation treatment techniques: 3D, 2D, and 1D.

3D dosimetry. Model-based algorithms. 3D dose distribution is a fast and accurate calculation within the patient in innovative radiation oncology. Calculations allow creating a reliable link between chosen treatment parameters and clinical outcome: geometry of irradiation fields, the prescribed dose for the tumor, etc. The treatment planning process has two main requirements: 1) it has to be fast (to fit in a time acceptable clinically) and 2) the results of the calculations have to be accurate and reliable. It is the main challenge between speed and accuracy of calculation developing dose calculation algorithms, especially for heterogeneous tissues (air cavities for paranasal sinuses, solid tumor for lung tissues. Model-based algorithms are implemented into commercially available and clinically used treatment planning systems (TPS). The pencil-beam algorithm is still the simplest and fastest dose calculation [11] more widespread, accurate, and sophisticated are superposition algorithms [12], which partly describe physical processes related to microscopic absorption of the energy delivered by irradiation. Almost all known physical aspects related to the microscopic radiation and tissue interactions are simulated using the Monte Carlo algorithm. Basic requirements for TPS [13-14]:

- Ability to simulate/ model the patient's body assessing tumor, internal organs, which are directly related to the irradiated area;
- Possibility to simulate/ model the geometry and doses of irradiation fields;
- Ability to observe the anatomical images, and the irradiation fields used for planning and the dose distribution in the irradiated volume (3D TPS).

Possibility to assess side effects (evaluation of dose-volume histograms – DVH). For example, if the total dose to the chiasma is 65 Gy per whol0e treatment, the percentage risk of blindness is 50 %, while 50 Gy/treatment, the risk is 5% [15].

3D gel dosimetry. Special attention today also is paid to an accurate dose verification technique, like monomer/ polymer gel dosimetry. This method is also known as 3D dosimetry and today it is known as the only "tool" used for the direct measurements of 3D dose distribution in irradiated volume (figure 3) [16].

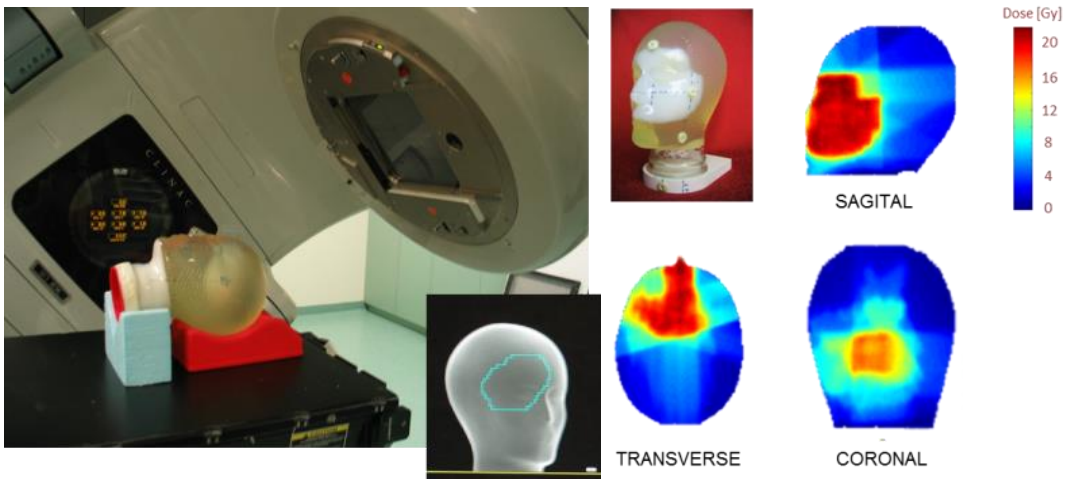

Fig. 3. Gel dosimeter phantom irradiated according to a conformal radiotherapy treatment (left side). The white region is the result of irradiation induced polymerization in the hydrogel. Maps of absorbed radiation dose are obtained by use of high-accuracy quantitative R_2 nuclear magnetic resonance imaging on a clinical MRI scanner (right side) [16]

Polymeric gel "dosimeters" are made of ionizing radiation-sensitive chemicals that polymerize upon exposure to radiation depending on the amount of absorbed dose.

The main advantage 3D gel dosimetry over ionization chambers (1D dosimetry) or radiochromic films (2D dosimetry) is measurements of three-dimensional (3D) dose distribution, especially it is important for the large dose gradients, which are specific for IMRT and VMAT techniques (tissue-equivalent Fricke gel dosimeters, have already been successfully used for the dose verification in IMRT and VMAT). Another advantage of polymeric gels is that due to the high water content in these gels, they do not require any energy corrections for electron and photon beams [17]. The only disadvantage of this method is that the gel could be used just once.

2D film dosimetry. Other methods like 2D or 1D dose measurements are limited, understanding and evaluating the absorbed dose distribution into the volume. 2D film dosimetry allows to analyze of the dose distribution in one plane (surface or in a certain depth), but it does not show full information about the dose distribution in a volume [18]. The 2D method is used to register irradiation doses with radiographic and radiochromic films (figure 4).

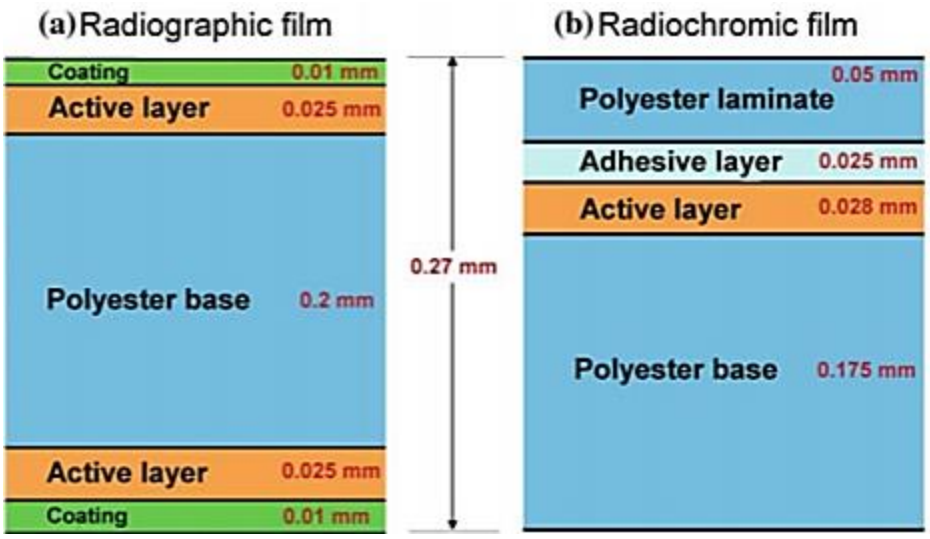

Fig. 4. Structure of the different dosimetric films [18]

An important part of these two film dosimeters is active layers/emulsions, which consists of AgBr and AgI crystals suspended in gelatin.

The radiographic film consists of thin plastic with emulsion gelatine coatings, which contains radiation-sensitive crystals a silver bromide (AgBr) [19]. The plastic base is coated with AgBr, which is after coated with the protective coating with gelatine on both sides of the film. The dose where the radiographic film is useful is ~2Gy, but the main advantage of using is that it doesn't perturb the beam [19]. When the photon interacts with the radiographic film, the electrons are released from the conduction band. Trapped electrons interact with Ag+. The ionization of AgBr creates the latent image in the film [19-20].

Radiochromic film consists of radiosensitive dye which polymerizes upon radiation exposure. The polymer is light sensitive, it changes the color when irradiation procedure. It measures the quantity of dose and provides 2D dose mapping. Compared to radiographic film, the radiochromic film can find a maximal dose but has lower sensitivity [19]. The film gets darker proportional to the absorbed dose [20].

Optical density usually is used for the intensity of the affected film by irradiation measurements. Optical density is defined as the logarithmic function of the incident intensity and transmitted intensity ratio:

$$OD = log_{10} \frac{I_0}{I}, \quad (1)$$

Even if the results of the measurements could be observed directly, some additional calculations and analysis have to be provided, and it could be done, for example using radiochromic films just after 48 h. [21].

1D dosimetry. The main disadvantage of 1D dosimetry is the ability to measure dose at one point. ***Thermoluminescent dosimetry.*** Thermoluminescence dosimeters (TLDs) are one of the most frequently used types of dosimeters, even if the dose is measured at one point. According to the small size of TLDs (mm row) and different shapes (powder, rod, chip, ribbon or disc), it could be placed in a tiny "cavities" (figure 5) [21].

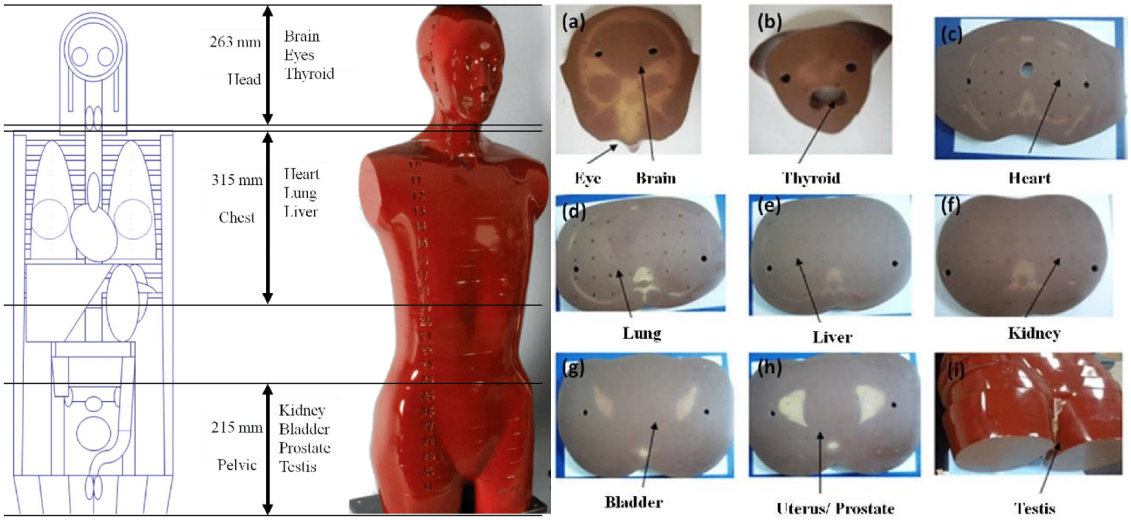

Fig. 5. Illustration of Rando phantom and the TLDs placed in a phantom slabs, according to the organs location at each slab [21]

Thermoluminescent materials (TL) used in a medicine, like beryllium oxide (BeO), lithium borate ($Li_2B_4O_7$) and lithium fluoride (LiF) [22-23] have a higher atomic number, while better sensitivity has aluminium oxide (AlO_3), calcium fluoride (CaF_2) and calcium sulphate ($CaSO_4$) [24-26], but all mentioned TL materials are nearly equivalent to the human tissue, could be reused for multiple time, and also, it is known, that TLDs response to the dose is linear in a large range. Also, it is known, that different materials have different response and sensitivity to ionising radiation [27-29].

Operation mechanism of TLDs is based on luminescence process. The incident ionising radiation alternates the structure of crystalline material. Therefore, an insulating material (TL material) absorbs a specific amount of energy and creates an electron-hole pair (mobile carriers). The electron then migrate towards the conduction band to the electron trap, while the hole migrate to a hole trap (along the valence band) (figure 5). The mobile carriers freely migrate in the crystal lattice until they are caught by traps (trapped in metastable states). Electron-hole pair combines at luminescent centres and releases light, when an external energy source (heat) is "transmitted" to electron and hole (to escape from the traps) [27-28].

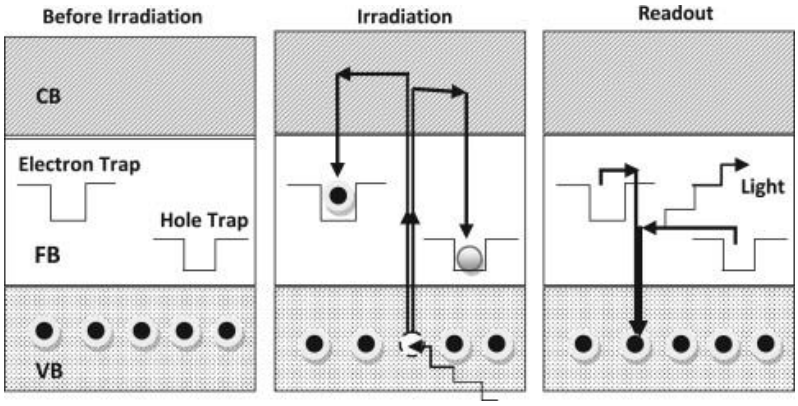

Fig. 6. The scheme of TL process: before irradiation, during irradiation and readout [27]

Ionization chambers dosimetry. The main guideline for external beam radiotherapy is published by International Atomic Energy Agency Technical Report Series (IAEA TRS-398) [30]. In this report the recommendations for absolute and relative dosimetry are provided for high energy photon beams (1 to 50 MeV), using ionization detectors (chambers) are provided. There are two types of cavity/ionization chambers depending on electrodes shape used in radiotherapy: 1) cylindrical (thimble) chambers and 2) plane-parallel (parallel-plate or flat) chambers. The most commonly used are cylindrical one with an active volume of 0.1 – 1.0 cm3. These types of ionization chambers are a gas (usually air) filled detectors, in which sensitive volume the electric field is applied. An electric field is formed applying a polarizing voltage onto two electrodes for collection of all charges created by direct ionization of the gas/ air. The produced electric current is usually a nano-amperes row. The amount of ionization produced by radiation is proportional to the mass of the sensitive volume. The air density (ρ_{air}) at the ambient atmosphere is a function of the temperature (T) and atmospheric pressure (p), which has to be corrected regarding the reference charge measurements conditions (temperature equal to 20°C (293.15 K) and a pressure – 101.325 kPa) [31]:

$$f_{pT} = \frac{1013.25}{p} \text{x} \frac{(T+273.15)}{293.15} \tag{2}$$

Therefore, the dose to air (D_{air}) in ionisation chamber cavity can be calculated from the basic relation:

$$D_{air} = \frac{Q_{air}}{\rho_{air}} \times \frac{W_{air}}{e} \tag{3}$$

where Q_{air} is measured charge in the air cavity; $\rho_{air} \cdot V$ is a sensitive air mass (m_{air}), then ρ_{air} is the air density in the cavity of the chamber and V is a volume of the cavity; W_{air}/e is the mean energy required to produce an ion pair in dry air (for radiotherapeutic photon and electron beams W_{air} is equal to 33.97 J/C), divided by an electron charge.

Such kinds of detectors/ ionization chambers seldom measure dose directly to the medium. It is known, that these detectors are created to "behave" as Bragg–Gray cavities in a high energy (megavoltage) photon and electron beams. The air volume of the ionization chamber is usually surrounded by a medium (most often it is water), for this reason relation of absorbed dose to the air in a cavity with absorbed dose in the medium could be explained using small size Bragg-Gray cavity theory (figure 7):

$$D_{med} = D_{air} \times \left(\frac{S^{SA}}{\rho}\right)_{med,\ air} \tag{4}$$

where $(S^{SA}/\rho)_{med,air}$ is the medium to air Spencer-Attix stopping power ratio (takes into account creation of delta (secondary) electrons, which are generated slowing the primary electrons) for the charged particle flounce spectrum present in the undisturbed medium [32].

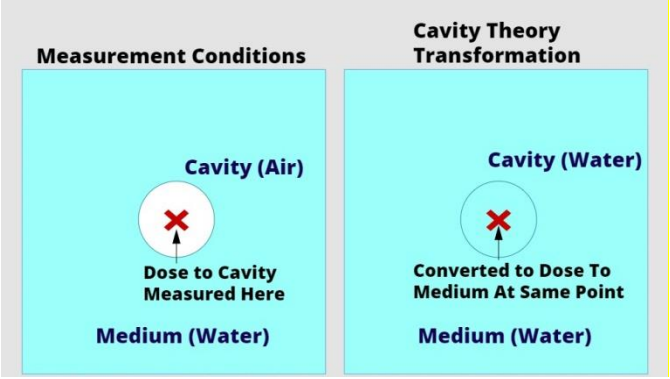

Fig. 7. Illustration of cavity theory [31]

Even if using ionization chambers the dose could be measured in one point, today it is the fastest, and simplest way to measure "directly" the dose.

Whatever the method will be used for the dosimetry measurements, it would not be performed without phantoms, i.e. imitators of the human's body.

Phantoms. The most often used phantoms in radiotherapy are water phantoms. The main requirements for this type of phantom are size ($30 \times 30 \times 30$ cm^3) (figure 8). Also, one important thing is, that if it is needed to perform measurements through the plastic wall (then the wall thickness is >0.2 cm) of the water phantoms, has to be accounted the density of wall [33].

Fig. 8. Small water phantom for absolute dosimetry [33]

Solid state phantoms. Standard polymethyl methacrylate (PMMA) phantoms (slabs or circular imitators of human body or head (figure 9), but it has limitation, they are expensive and it has homogeneous geometrical structure [34].

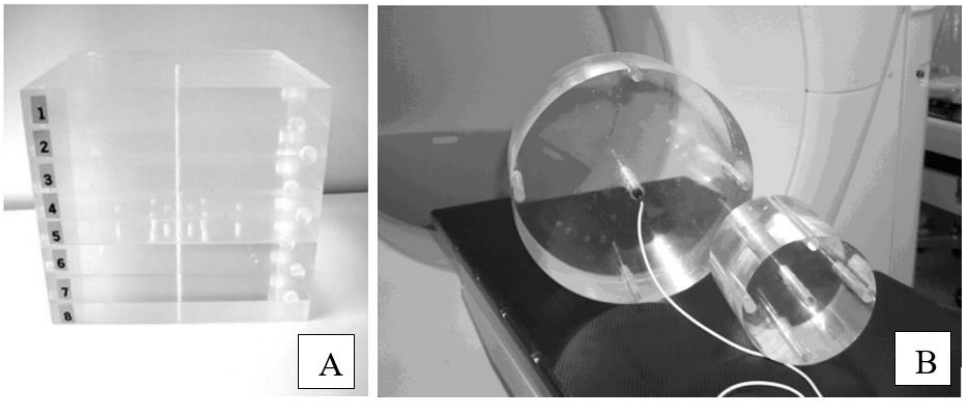

Fig. 9. Standard polymethyl methacrylate (PMMA) phantoms, A – slabs, B – circular immitation of human body or head [35-36]

The main disadvantage of water phantoms and already mentioned solid state phantoms, that they cannot imitate the realistic processes of treatment procedures. Therefore, anatomical models are very important in dosimetry, as it is not possible/ almost impossible to measure directly the absorbed doses in living human organs, and direct invasive studies are dangerous to human health. According to this physical anthropomorphic phantoms are successfully used in clinical practice.

Anthropomorphic (realistic) phantoms. Also, it could be used so-called anthropomorphic phantoms, like RANDO Alderson phantom (figure 2), which represents the human body equivalent phantom and consists of bone and tissue-equivalent materials emerged in a phantom [37]. This type of phantom is divided by slices/ slabs, in these slabs the TLD dosimeters are possible to place. RANDO phantoms might represent the newborn child, also toddler (1-3 years

old kid) and child (3-7 years old) [37], as well as male and female adult patients [38]. Such kind of phantoms is implemented in radiation therapy practice, due to the high accuracy.

Today then 3D printing technology becomes more and more popular, due to its low cost and efficiency of 3D patient-specified anthropomorphic phantoms are started to be widely used in medicine (figure 10) [39].

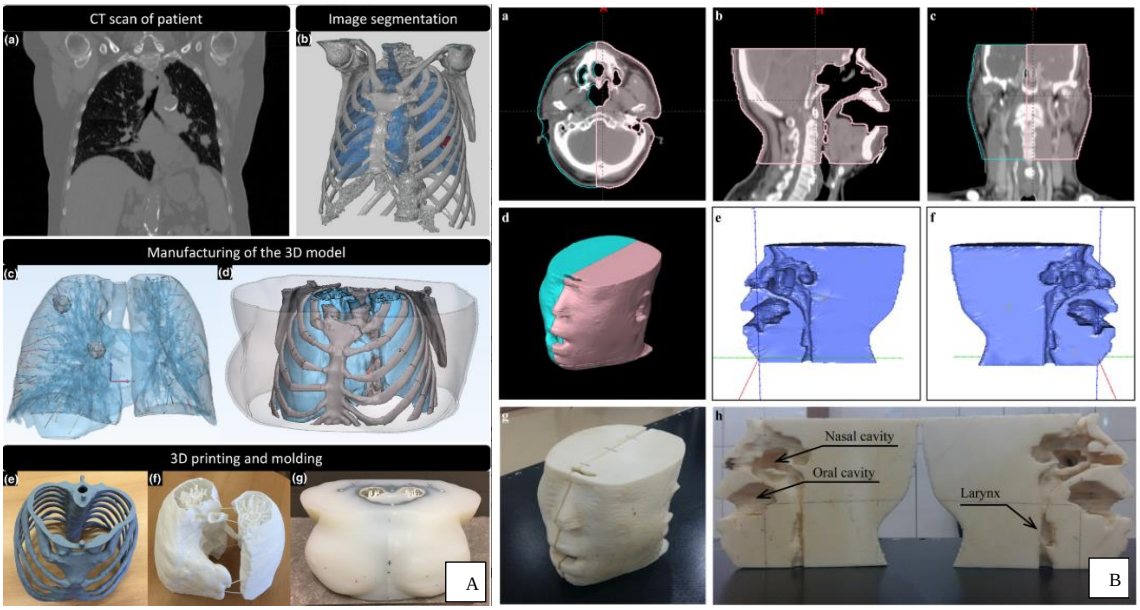

Fig. 10. 3D patient-specified anthropomorphic phantoms for breast (A) and head and neck (B) [40-41]

This technique is fast, enough cheap, and allows for medical staff to work efficiently performing patient dosimetry and minimize the possible errors evaluating the absorbed dose in a volume related to the complex geometry or different densities inside the body [34], especially then it is possible to imitate patient's real organs and geometry issues.

Dosimetry methods and phantoms used in clinical practice it is not the only issues, which helps to ensure the quality of the treatment outcome, especially if such cases, like shallow tumors (lymph node metastasis, nasal cavity, and paranasal sinuses, end, etc.) or irradiation of uneven and concaved surfaces has to be irradiated using a high energy photon and the maximum prescribed dose has to be delivered for the surface tissues as well, but due to skin-sparing effect, it is not able to do [42]. For this reason is used so-called compensators and boluses, which are briefly described in the next 1.3. Chapter.

1.3 Compensators and Boluses in external beam radiotherapy

It is known, that the dose on the patient's surface to a certain depth of dose maximum depends on irradiation field size and source surface distance (SSD), i.e. smaller size of the field and larger SSD, the dose on the surface is smaller. Such kind of the dose distribution on the surface determines reactions of the skin, which depends on the energy of the field and the depth of the tumor, i.e. deeper the tumor, higher energy of the photons has to be chosen. Dependence of the dose changes within the depth in water is shown in Figure 11.

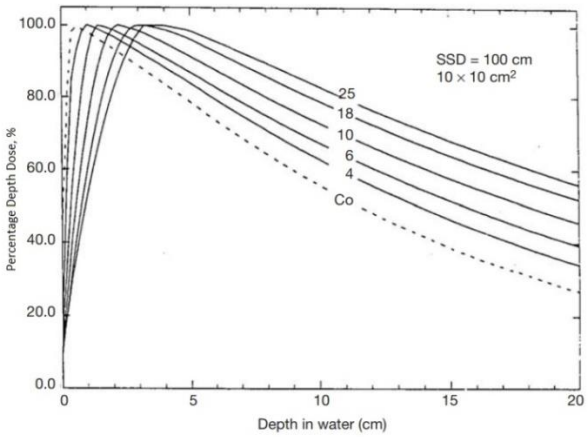

Fig. 11. Percentage depth dose dependence on the depth in water, then energy of the field changes [43]

Percentage depth dose (PDD) in a patient's body (in a volume) depends on beam energy and size of the field is showed in a Figure 12: then irradiation dose and energy is constant, photons penetrate deeper, if size of the field is larger [43-44].

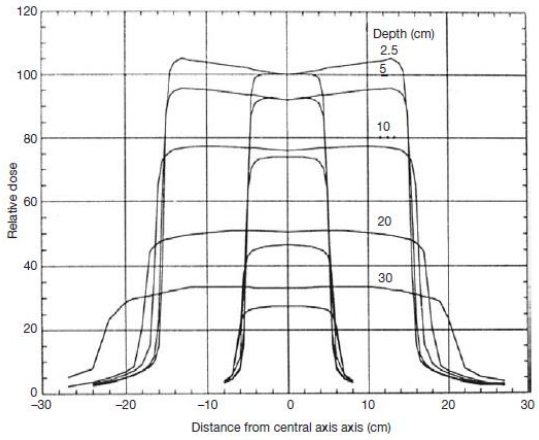

Fig. 12. Depth dose dependence from the size of field (10 cm × 10 cm and 30 cm × 30 cm), then the energy of photons is equal to 10 MeV [1]

Therefore, using high energy (MeV) photons due to skin sparing effect irradiating shallow tumors, this effect could be reduced, using an additional "tools", like compensators or boluses (figure 13).

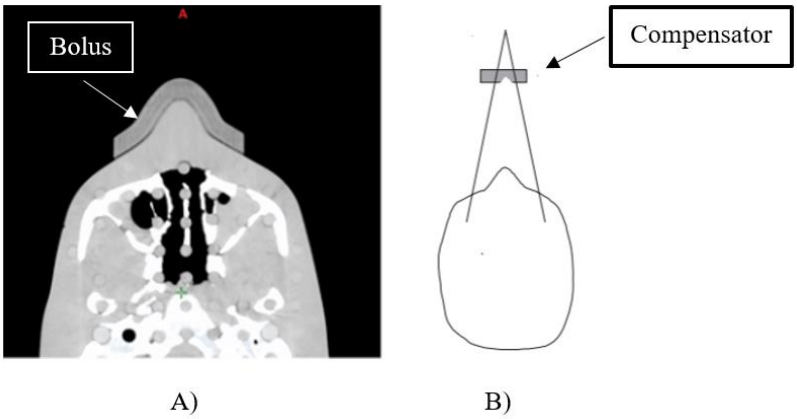

Fig. 13. A) 3D printed patient-specific bolus [1] and B) compensator [45]

Additional tools leads to a better quality of treatment outcome, avoiding the possible risk of recurrences, if the tumour is located near the surface [1, 45-46].

1.3.1 Compensators

As it is known, using a compensator, it is possible to curve shapes and irregularity of human body causes, creating the non-uniform isodoses distribution into the volume [47, 48]. It is placed on the distance from the patient and compensates "missing tissue", so reducing the scatter of irradiation at the various depths and ensuring a uniform isodoses distribution in an irradiated volume (figure 14) [47]. The materials used to create a compensator could be: tungsten powder in mold, tin or steel granule in mold, tin granule wax mixture in mold, brass, still, lead, etc. [48]. Today, more and more frequent compensators are fabricated, for example, using a 3D printing technique: 1) mold is printed using the 3D printer; 2) a wax is heated, when it becomes liquid it is mixed with tungsten powder; 3) all the mixture is poured in a 3D printed mold and cooled down in the room temperature; 4) after it's cooled down the compensator is removed from the mold and is already ready to use [43].

Therefore, if the compensator is placed in a distance, the bolus is placed on the patient's surface and creates a dose build-up region on the patient's surface.

Compensators are widely used for the post-mastectomy patients, compensating missing tissues on the scar and uniform the isodoses distribution, but also it is one of the tools creating a more uniform isodoses distribution in a volume and compensating missing tissues of the patient's body for H&N cancer cases (figure 13 and figure 14) [47].

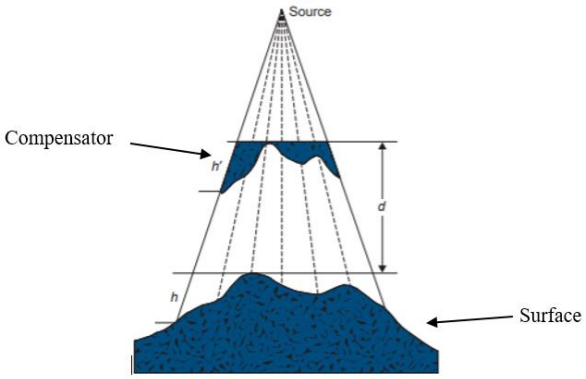

Fig. 14. Illustration of compensator for the irregular surface: h' – thickness of the compensator that is equal to the height (h) that is needed to uniform the isodoses distribution on the surface [47]

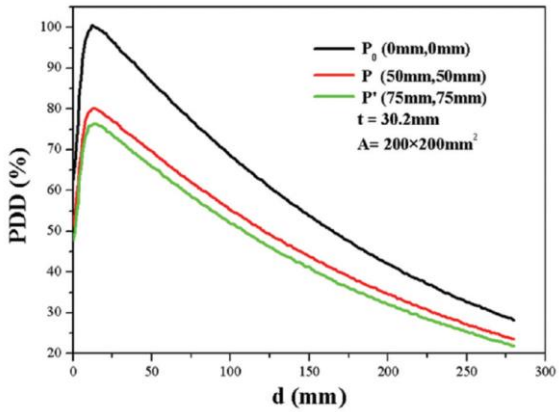

Fig 15. Percentage Depth Dose (PDD) per distance mm, during 6MV photon energy IMRT treatment, by using 30.2 mm thickness cadmium-free compensator with field size 200 mm^2 x 200 mm^2 at off-axis points (penumbra) P_0 (0mm,0mm), P (50mm, 50mm) and P' (75mm, 75mm) [44]

1.3.2 Boluses

The bolus is a human body equivalent material, which is placed directly on the patient's surface as an additional body [47].

Since irradiating near-surface tumors with high energy photons creates a lack of the dose on the surface, boluses play an important role as an additional body layer, which results in a better homogeneity and conformity of the dose to the body surface [49]. So the application of bolus in radiotherapy compensates missing tissues, leads to better treatment quality, avoiding the risk of possible recurrences, also helps to create homogeneous dose distribution on the patient's surface/ skin [50]. M. J. Butson, etc. [2] study showed, that dose distribution in different depths is influenced with the use of the bolus and how it depends on the size of the field (Figure 16). The results showed, that the surface absorbed dose without bolus for 8 cm × 8 cm irradiation field is equal to 14 %, while for 10 cm × 20 cm – 21 %, while using 1 cm thickness bolus, the surface an

absorbed dose increases respectively to 98 % and 99 %. The results show, that using a bolus it is possible to create absorbed dose maximum on the surface/ skin.

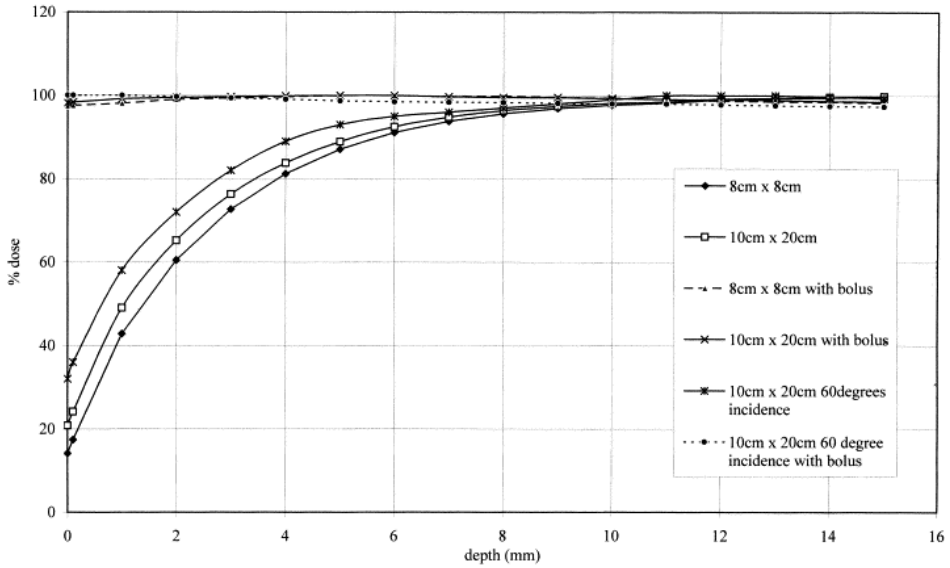

Fig 16. Percentage depth dose distribution with and without bolus: photon beam energy 6 MeV; gantry angles 0° and 60°; SSD – 100 cm; field sizes: 8 cm × 8 cm and 10 cm × 20 cm [2]

Therefore, build-up material (bolus) has a vital implementation in electron beam and photon radiotherapy, as they are used for many types of shallow cancer treatment, expecting an important improvement of treatment procedure outcome, so ensuring better control of the disease. The bolus usually is used as an additional body for a post-mastectomy, but also it could be used and for H&N and other types of shallow cancer localizations, in order to "compensate" missing tissue during irradiation procedure, creating a maximum prescribed dose on a patient's surface/ skin [49-52]. M. Fischbach, etc. [53] study showed, that using 0.5 cm thickness silicone bolus for 6 MeV irradiation in compare with results without bolus, dose in 1 mm depth increased from 76.7 % to 84.7 %, while in 3 mm depth dose increases from 93.0 % to 95.7 %. Therefore, the treatment of shallow tumors, using the bolus is effective and improves treatment outcomes significantly. However, So-Yeon Park, etc. [50] showed, that irradiating a scar the bolus also can be used as some sort of "shielding material" for organs at risk (OAR), like heart and lung, because it minimizes dose (so decreases Normal Tissue Complication Probability (NTCP)) for the healthy tissues and OARs, optimizing an isodoses distribution in a volume. How it looks like isodoses distribution in a volume, then is used so-called bolus as a "shielding material" for the OARs, like left kidney, it could be seen in figure 17.

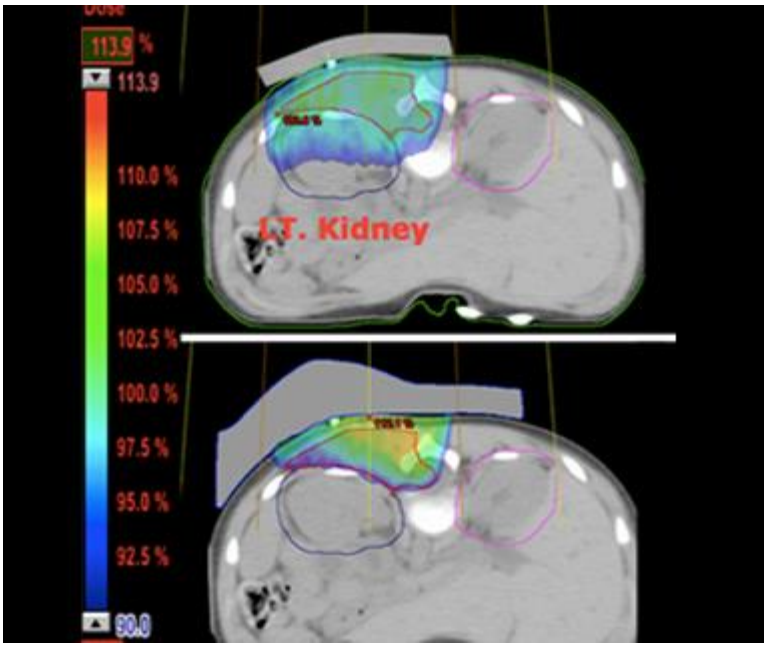

Fig 17. Isodoses distribution in a body using different geometries of the boluses [54]

The most usual material used for bolus fabrication in daily clinical practice is silicone [55]. The main characteristics of the silicone there are: flexible, it is easy to store, to use, cost-effective, non-toxic, and is tissue equivalent. However, it is known, that even if the standard flexible silicone bolus is used during treatment procedures, in most cases it would be impossible to avoid air gaps between the patient's body and the bolus [49-56]. M. J. Butson and co-authors [2] study showed, that using bolus air gaps of 4 mm reduces the dose of approximately 4 % for basal layer and depends on field size and angle of incident, while air gaps of 10 mm, reduce the dose up to 10 %. So the main conclusion is, that air gaps should be minimized or avoided as possible. It is known, that it is possible to minimize or avoid air gaps using, for example, "sticking" silicone bolus (silicone by itself is a sticking material, so one side of the bolus were used to be without plastic cover, which is usually used to), which sticks on the patient/phantom surface [56]. This type of bolus showed better results in comparison to a standard silicone bolus: air gaps were minimized (from 5 mm to 3 mm) or even avoided. Another alternative for the standard or "sticking" silicone bolus is to use individualized 3D printed bolus [57].

3D printed boluses. Different printed issues, like parts of the phantoms or even whole phantoms, mold of compensators, boluses using the 3D printed technique is a quite new "tool" in a radiotherapy field, accordingly to this today, is paid a lot of attention investigating properties of the used materials and possibilities to use printed issues in clinical practice [58, 61]. A choice of materials used for printing requires a long time of evaluation of the properties and characteristics [58, 61]. The main question is how to choose the most suitable? Using 3D printing technique in clinical practice, it is very important to pay attention to the main characteristics of used materials, like density, equivalency to a human body (tissues/ organs), attenuation properties, which could

be evaluated using CT number values Hounsfield units (HU) [58]. HU is proportional to the photons attenuation coefficient in the human body, which is expressed on the greyscale, where -1000 is air (totally black) +1000 is bone (totally white) (figure 18) [59-60].

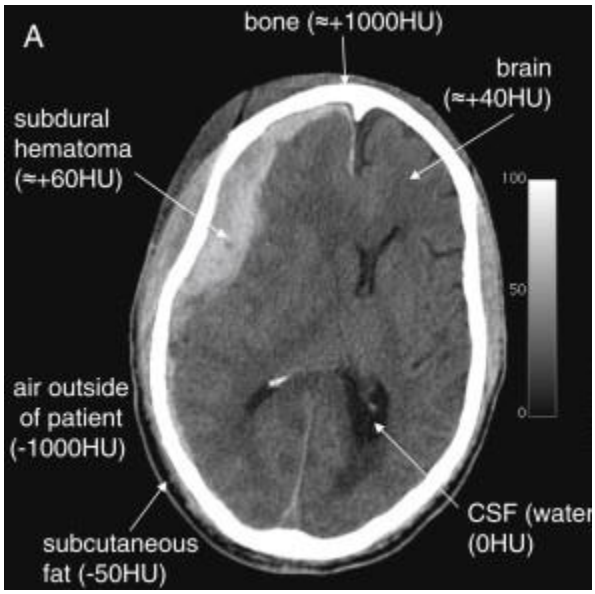

Fig 18. Grey scale expression of HU values on the head CT. Bone ~+1000 HU, the air outside the patient is -1000 HU [60]

For example, 3D printed materials, like Polylactic acid (PLA) and Acrylonitrile butadiene styrene ABS [58] are human tissue equivalent, as well as standard silicone [62]. Also, it is known, that PLA and ABS could be used to print for example, for head, thorax surface areas, while acrylic polymer – used to print spine, and etc. (table 4) [58].

Table 2. Characteristics of the main 3D printing materials used in a clinical practice

3D printed materials	**Chemical formula**	**3D printed material density, g/cm^3**	**Anatomic structure**	**Anatomic structure density, g/cm^3**
Polylastic acid (PLA)	$C_3H_4O_2$	1.01-1.43	Thyroid gland/ Skin/ Bone	1.045/ 1.09/ 1.92
Poly(acrylonitrile-co-styrene-co-acrylate) (ASA)	$C_{15}H_{17}NO_2$	1.06-1.10	Brain	1.05
Glycol-modified polyethylene terephthalate (PETG)	$C_{16}H_{28}O_8$	1.27	Bone	1.92
High impact polysterene (HIPS)	$C_{12}H_{16}$	1.04-1.05	Muscle	1.04
Acrylonitrile butadiene styrene (ABS)	$C_8H_8•C_4H_6•C_3H_3N)_n$ [63]	1.04 [63]	Bone [63]	1.92 [64]

As it was already mentioned, that silicone bolus is a soft and flexible, while 3D printed bolus is a

solid state (figure 12), but due to ability print it individually for each patient, printing technique appeared to have a wide scope of view, creating an individualized phantom or bolus specified for the patient characterized shapes [2-65].

Fig 19. A) silicone bolus (image was taken from French manufacturer Arplay commercial bolus - Bolusil®) and B) 3D printed bolus [1]

"Dosimetrical" aspects of the 3D printed boluses used in external radiotherapy. The main advantage of 3D printed bolus, in comparison with a standard silicone bolus it is possible to avoid or minimize unwanted air gaps much more, that means absorbed dose under the bolus and isodoses distribution in a volume are more accurate. Due to fallowing reasons individualized 3D printed, for example, PLA bolus proves its reliability using it in the clinical practice. K. Fujimoto and etc. [1] made study which showed, that 3D printed ABS bolus had a good clinical outcome at any thickness, which differs from 0.5 cm to 3.0 cm, especially paying attention to the air gaps created in between "patient" and bolus (Figure 19).

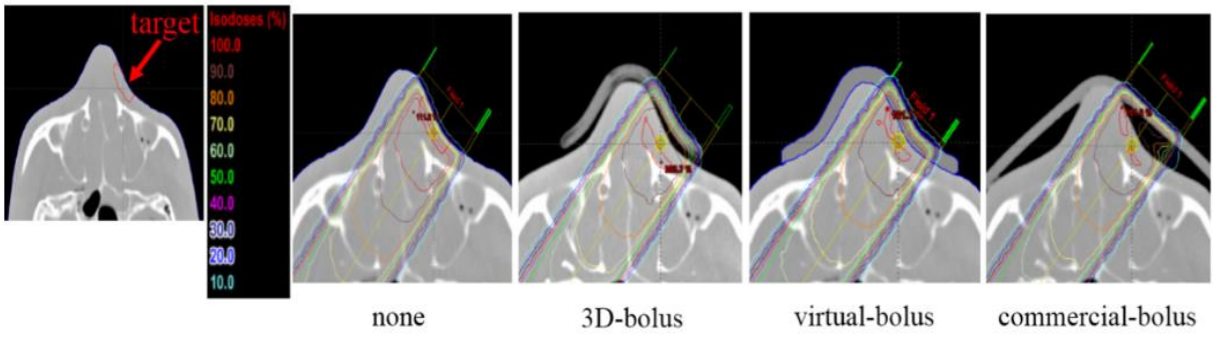

Fig 20. Dose distribution showed for four treatment plans, using three different types of 0.5 cm boluses: 3D printed bolus, virtual bolus (created with treatment planning system) and commercial bolus [1]

Therefore, it was concluded, that using 3D printed bolus has benefits for the patients and for medical staff, because it ensures better accuracy in set-up process, saves the time of designing bolus, it is easy to produce, which has high accuracy in delivering dose and reduces air gaps while

applying on the irregular surface of the patient body (head and neck) [1]. During the study done by Kim SW. [1] there was used 2 boluses: standard and customized 3D printed, where was observed, that using standard bolus resulted in an unwanted air gap, which was minimized and/ or avoided using customized 3D printed bolus, especially on concaved surfaces (Figure 21). Results of this study showed, that the 3D printed customized bolus has better dose distribution and better fitting with irregular surfaces [1].

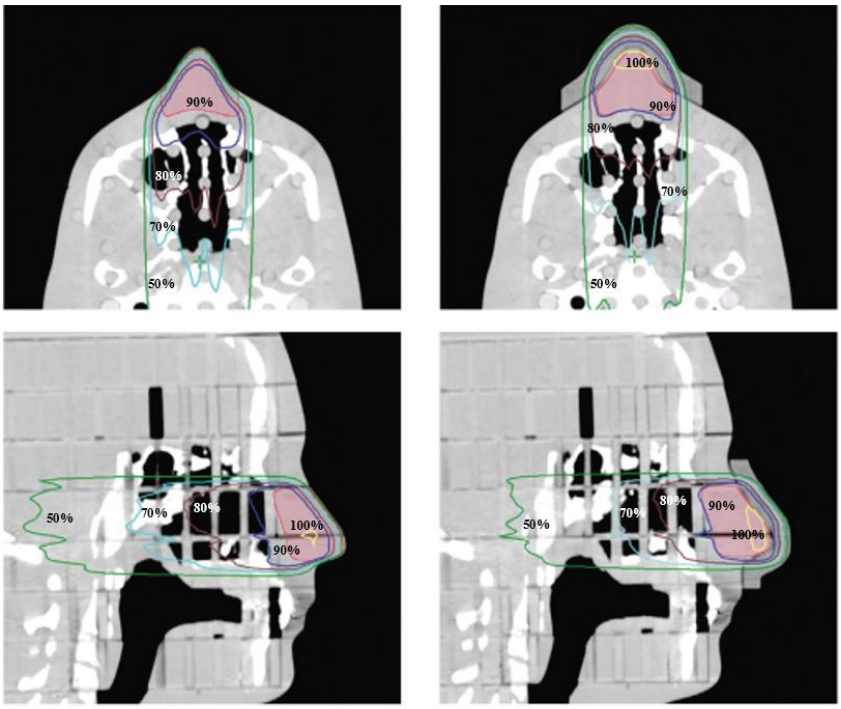

A) B)

Fig 21. Dose distributions of the two irradiation treatment plans using the RANDO phantom: A) plan without bolus, B) plan with the 3D printed bolus. Yellow line, 100% isodose contour; blue line, 90% isodose contour; brown line, 80% isodose contour; cyan line, 70%isodose contour; dark green line, 50% isodose contour [1]

However, the main challenge starting to use 3D printing boluses it is not enough to choose material and print a bolus, it is a complex procedure (reconstruction of the images, printing technique issues, like infill ratio and etc.), which influences a successful use of individualized 3D printed boluses in clinical practice.

1.4 The main aspects of 3D printing technique

One of the criteria's, which affects individualised 3D printed boluses appropriate use in radiotherapy is infill percentage of printing material (infill ratio or infill density), which depends on chosen infill patterns as well. The material density may vary with different infill patterns due to different material distribution during the printing (figure 22).

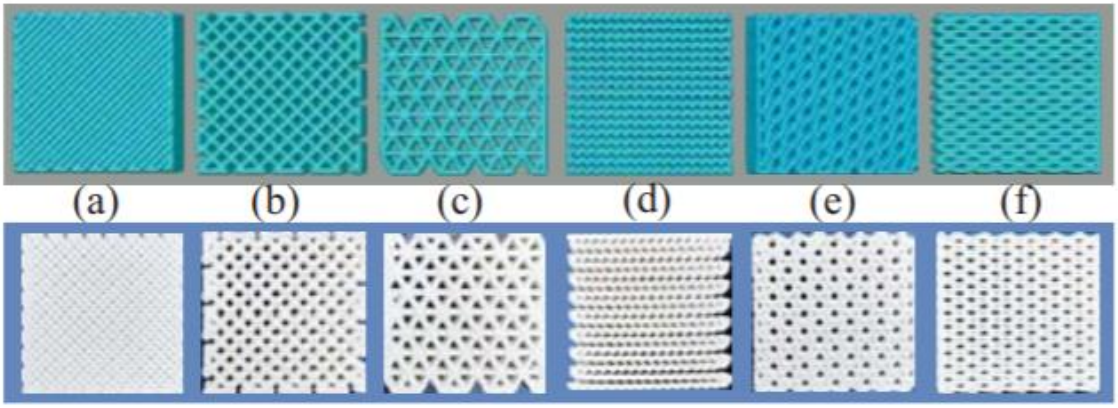

Fig 22. Illustrative and actual structures of typical infill patterns. (a) rectilinear, (b) grid, (c) triangular, (d) wiggle, (e) full honeycomb and (f) fast honeycomb. All the samples infill percentages are set to 90% in the printer software [66]

According to a study done by Z. Moghaddam and et. al. [54] the printing infill is tremendously important for homogeneity of material and the conformity of dose distribution. In this study different infill percentages, PLA boluses were evaluated (from 20% to 100%) and irradiated with 6, 8, 10, and 12 MeV electrons energies. The results showed, that that higher the infill percentage means better homogeneity of the object (bolus). Analyzed percentage depth dose curve of 100% infill PLA bolus has the best correspondence with percentage depth dose in water. Therefore, it means that a 100% infill ratio has the best dosimetric results compared with lower infill density (20%) boluses [54]. The other study was done by R. Ricotti and et. al. [67] evaluated 3D printed PLA and ABS boluses with different infill density. In this study the boluses were printed with rectilinear mesh pattern with a different infill percentage boluses – 10%, 20%, 40%, 60%, irradiating them with a single field (field size 5 cm x 5 cm) treatment plan using 6 MeV photon energy beam (figure 19) [67]. It was found, that higher infill density bolus (PLA bolus had higher density compared to ABS bolus at the same infill percentage) with higher homogeneity of the material corresponds the better homogeneity of dose distribution for maximum 6 MeV photon energy, while with 40% and 60% infill densities printed boluses showed 5% difference on the measured dose distribution (figure 23) [67].

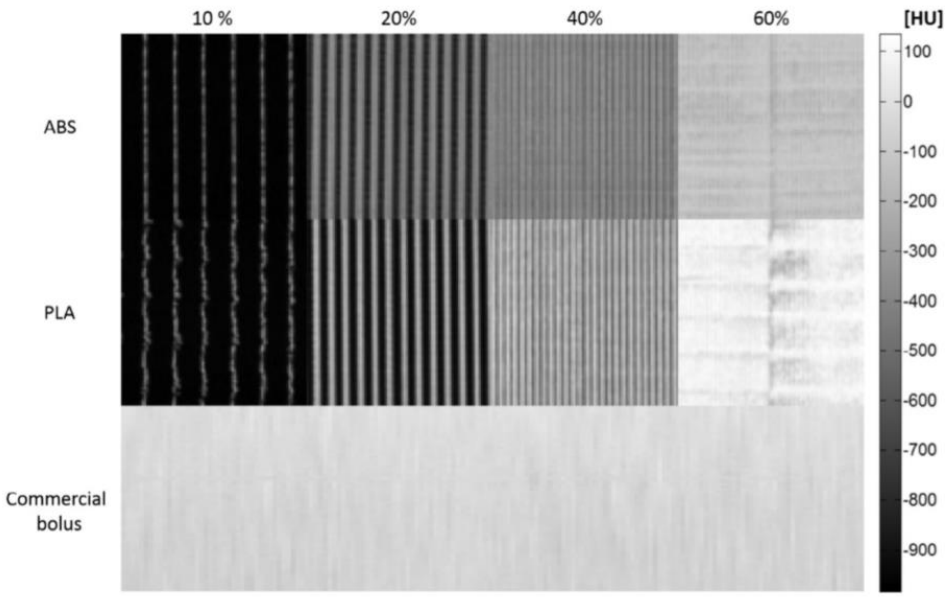

Fig 23. CT scans of the analysed boluses. The internal structure (infill pattern) of the 3D printed (PLA and ABS) and the commercial bolus is visible. The colour bar refers to the Hounsfield Units (HU) measured by the computed tomography (CT) scan [67]

According to the analysis of the film dosimetry results regarding to infill ratio showed, that under 100% infill ratio bolus homogeneity of the dose distribution on the surface (figure 24 A) is not influenced by the pattern of the 3D printing, and it could be successfully used for 2D films dosimetry. However, attention should be paid to a "patterned" dose distribution under the bolus (figure 24 B), using a 90 % infill ratio. This resulted in additional uncertainties in dose delivery to the patient. Due to this reason it is recommended to use bolus printed with 100% infill ratio, assuring more reliable dose measurement using 2D film dosimetry. Films dosimetry reviled, that the infill ratio plays important role using printing issues for medicine applications [49].

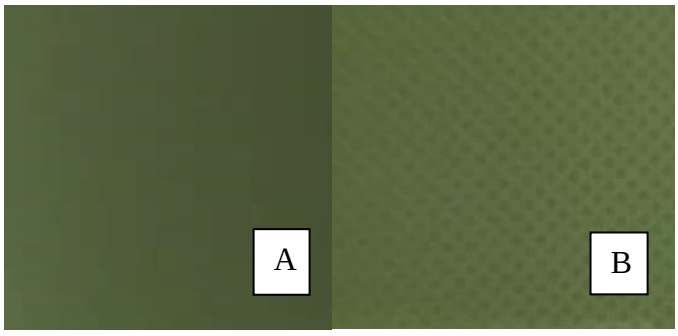

Fig 24. 2D GafChromic films EBT2 irradiated between the standard CT PMMA head phantom and the 3D printed polylactic acid plastic (PLA) bolus. A – irradiated GafChromic film under the 100 % infill ratio 3D printed PLA bolus. B – irradiated GafChromic film under the 90 % infill ratio 3D printed PLA bolus [49]

Summary of literature review

Radiotherapy aims to protect healthy organs while irradiating the tumor. Head and neck are one of the most common cancer localization with close vicinity of organs. For this reason a lot of methods have been developed to control the irradiation doses on the critical organs. Nowadays the science cannot answer the question of what stochastic or deterministic effect may cause to the living tissue. As a result, a lot of methods are developed to control the possible risks to the critical organs.

Quality assurance (QA) and quality control (QC) assures the accuracy of dose delivery with minimized errors. To perform quality assurance and quality control dosimetry is the main method. Dosimetry is considered as one of the most efficient tools in everyday practice in radiotherapy. 1D, 2D, and 3D dosimetry methods help specialists control the dose to the critical organ and tumor in order to avoid unjustified irradiation. The measurements of irradiation doses are taking place on the surface of the patient's body, but in some cases the dose distribution on the deeper localizations is required. For this reason the phantoms are used. Different types of phantoms imitate the different parts of the human body (whole body, head), which help specialists check the delivered doses to the tumor and the OARs.

Irradiation of superficial lesions using high-energy (MeV) photons beam creates a skin-sparing effect that switches isodose to the deeper localizations, which means treatment failure, due to the irradiation dose is delivered to the critical organs, not to the target volume (TV). The solution to overcome this problem is boluses. 3D printing technology is highly implemented in creating individualized boluses for the patients. Commercially available boluses create the air gaps between the bolus and the patient surface and the dose distribution becomes inhomogeneous and decreases as the air gap occurs. 3D printed boluses minimized the existence of air gaps between the bolus and the patient's surface.

The 3D printing technique is a new method in radiotherapy which improves the optimization of radiotherapy procedure

2 Materials and methods

Two different thickness (0.5 cm and 1.0 cm) of individualized 3D printed polylactic acid (PLA) boluses were used imitating irradiation of shallow head and neck cancer with a high energy photons (6 MeV energy usually is used for head and neck cancer irradiation). It is known, that the main problem using boluses in radiotherapy ensuring the better treatment outcome is air gaps formed between bolus and patient. For this reason, the patient-specific phantom was fabricated, attaching 3D printed PLA middle part of the face (eyes and nose region) reconstructed from the CT images to a surface of the standard computed tomography (CT) polymethyl methacrylate (PMMA) head phantom (figure 21). The detailed process of reconstruction and 3D printing is described in 2.1 chapter "Reconstruction and 3D printing of the patient-specific phantom and individualized bolus".

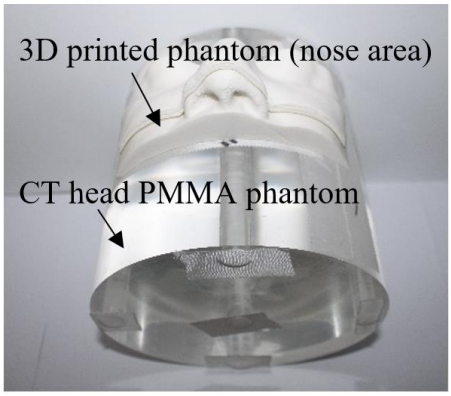

Fig 25. CT PMMA phantom, 3D printed PLA phantom

2.1 Reconstruction and 3D printing of the patient specific phantom and individualized bolus

Patient specific phantom and individualised bolus reconstruction and creation process consisted from these steps:

1. ***Real patient's reconstruction creating patient's 3D model.*** Reconstruction was done in cooperation with PhD student Antonio Jreije (KTU) from computed tomography (CT) images, using the open platform software program "3DSlicer" (figure 26). "3D Slicer" is used to transform the computed tomography scans into a 3D digital format (figure 26B), creating a model of an object.

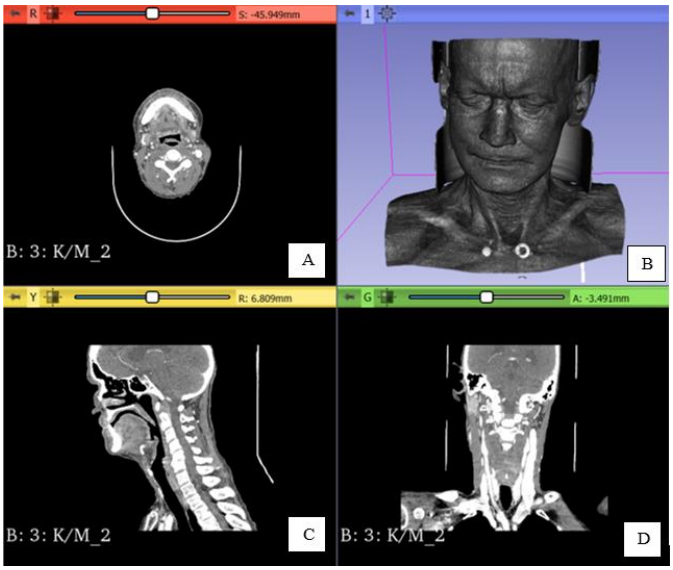

Fig 26. Interface of free software platform "3DSlicer". Patient's reconstruction from computed tomography (CT) images, creating a 3D model (B)

The program "3D Slicer" allows to manipulate whole image removing or adding structures, like bones or soft tissue, also slicing images/model into different directions (figure 26).

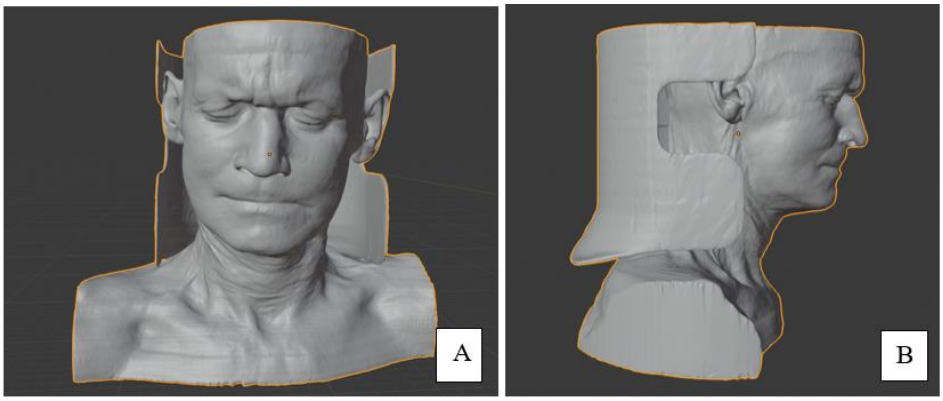

Fig 27. Reconstructed patient's 3D model from CT scans. A – the longitudinal view of the patient; B – the transverse view of the patient

Creating patient's 3D model, DICOM (Digital Images and Communications in Medicine) [67] file has to be uploaded and combined with the special functions in order to get a 3D model of the patient, afterward this file has to be converted to stereolithography (STL) file [67]. STL file of the reconstructed 3D model from patient's CT scans was used to create a patient-specific phantom for the middle part of the face (eyes and nose region), using the free software program "Blender" (Figure 27).

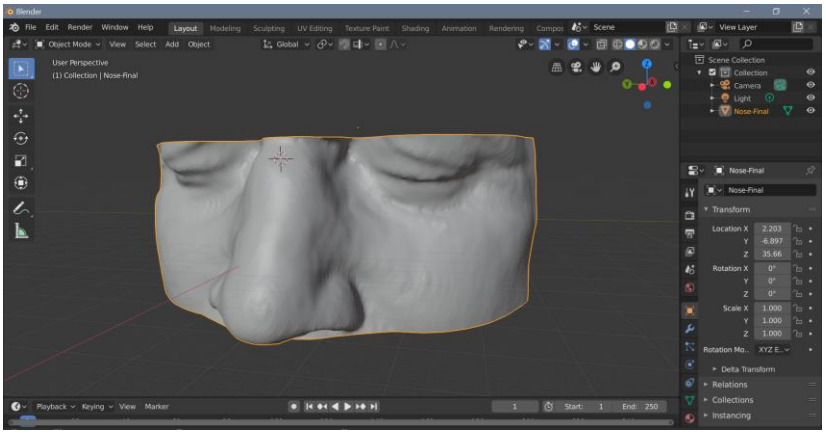

Fig 28. Interface of the program "Blender"

2. ***3D printing of reconstructed patient (middle part of the face) from polylactic acid (PLA) material (was done by PhD student Antonio Jreije (KTU))***, attaching/ fixing it to the surface of standard polymethyl methacrylate (PMMA) CT head phantom (figure 29).

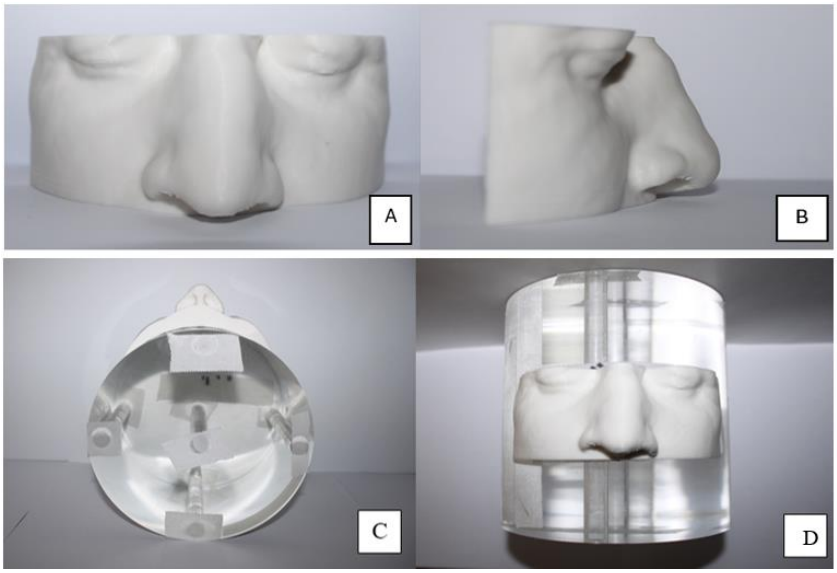

Fig 29. 3D printed middle part of the face. A – The longitudinal view of the 3D model of the phantom; B – the transverse view of the 3D model of the phantom; C and D – attached 3D printed model to the PMMA CT head phantom

Printing process of patient specific phantom consisted from these steps:

a. Reconstructed 3D model of the bolus for the ***review*** were uploaded into the program "Print 3D" (figure 30).

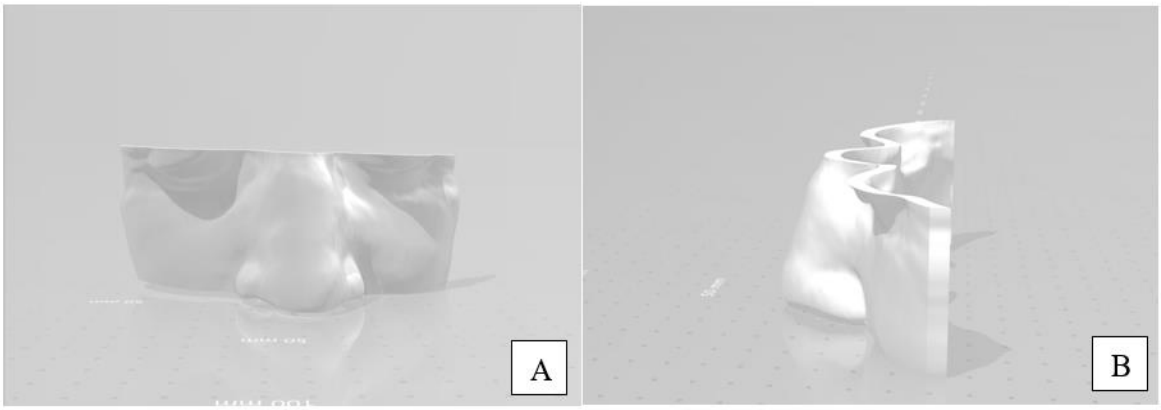

Fig 30. The program "Print 3D" shows the approximately final result. A – longitudinal and B – transvers view

b. *Printing.* Printing was performed using a software program "Z-suite" (figure 31) and printer "Zortrax M300 3D".The patient specific phantom and individualized boluses were printed in Kaunas University of Technology, Department of Physics (figure 29).

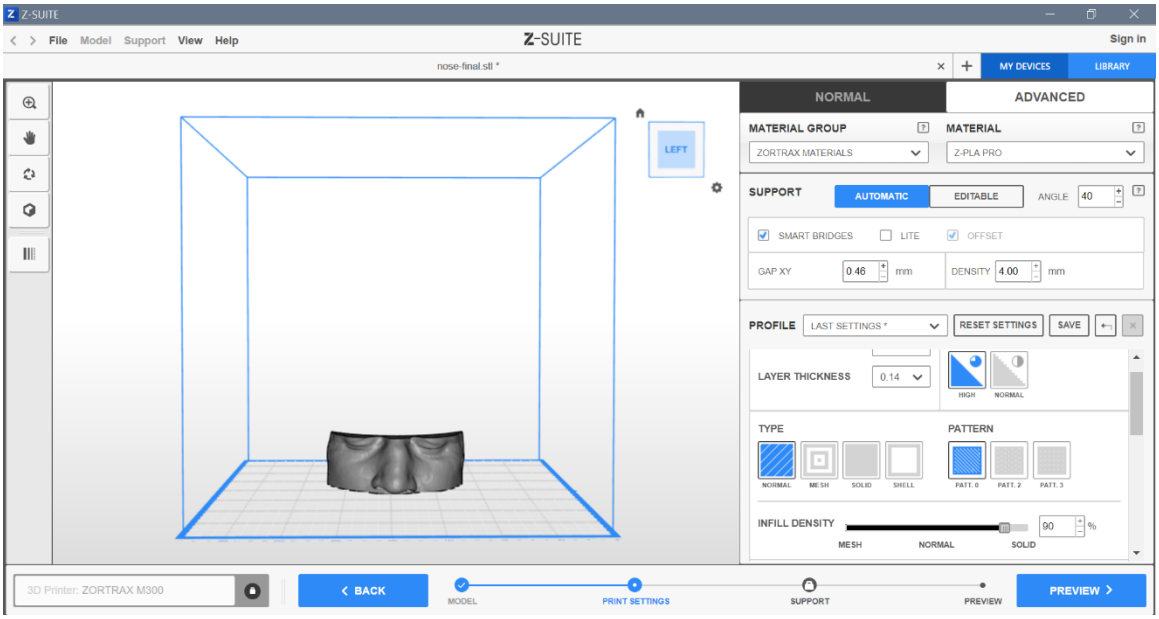

Fig 31. The program Z-Suite, which shows the printing parameters

The patient specific phantom was printed using polylactic acid (PLA) filament, with 90 % infill ratio. It was found, what using for printing 90 %infill ratio for the patient specific phantom it showed a good agreement with a soft tissues Hounsfield unit (HU) values, taken from the head and neck cancer patients' facial region CT images (figure 32).

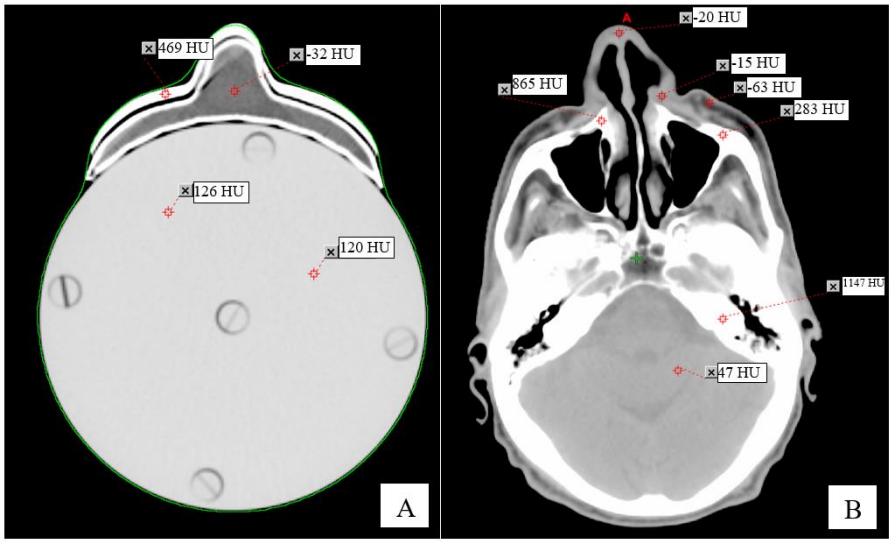

Fig 32. A – HU values of the 3D printed bolus, PMMA phantom and 3D printed part of patient specific phantom; B – H&N patient HU values chosen for different patient's organs (bone, scull, soft tissues and brain)

3. ***Bolus reconstruction (figure 21 C and D) and 3D printing,*** from the CT scanned patient specific phantom (figure 21 A and B), following the same principle like in the first step "patient's" reconstruction was done.

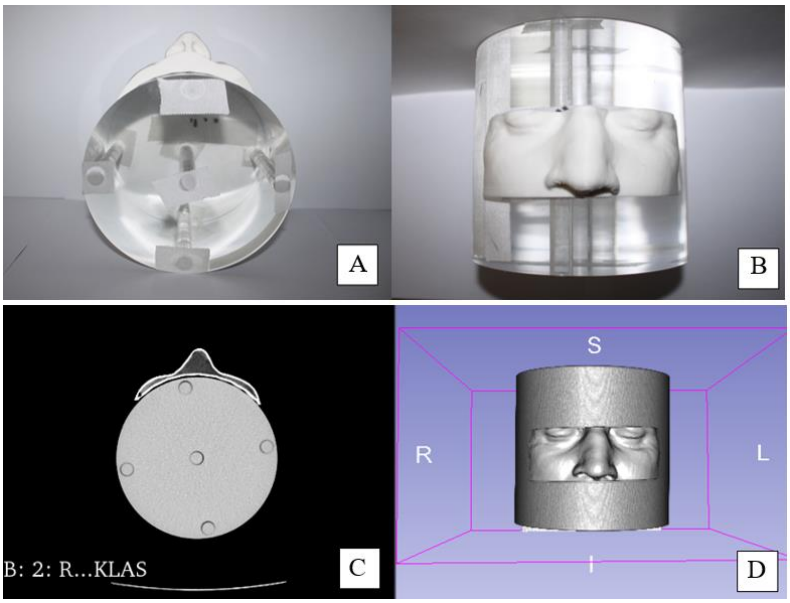

Fig 33. A and B – patient specific phantom; D – reconstruction of the patient specific phantom from the B – CT scans

Two different thickness (0.5 cm and 1.0 cm) boluses were recreated on a program "Blender" using 3D printed patient specific phantom (figure 29 and figure 34) and printed. 0.5 cm and 1.0 cm thickness were chosen regarding to photons energy (6 MeV) used imitating shallow head and neck

(H&N) cancer irradiation procedure. It is known, that the maximum dose depth of 6 MeV photons is 1.5 cm, so usually 1.0 cm thickness bolus is used. However, some studies showed, that 0.5 cm bolus ensures the sufficient dose distribution on the patient's surface, irradiating with 6 MeV photons [52, 1]. Due to this reason in this research project two different thicknesses boluses were analysed.

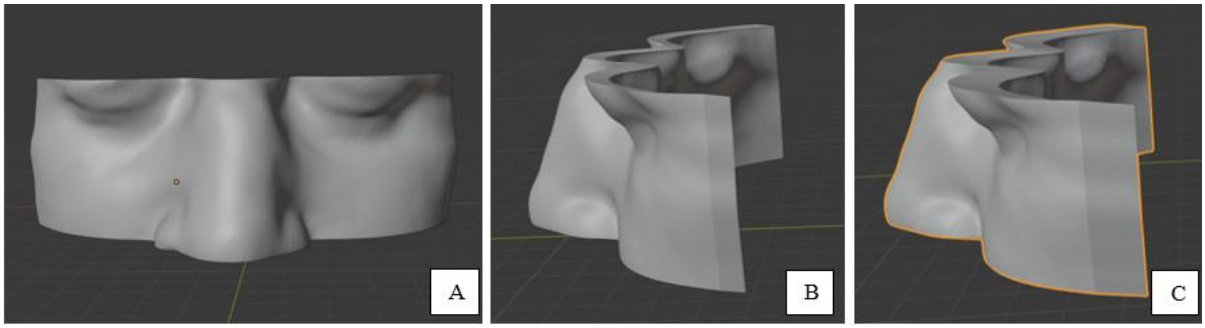

Fig 34. Reconstructed bolus with diameter 1cm was recreated out of scanned 3D printed specific patient PLA phantom. A – Longitudinal, B and C – transverse view of 3D modelling of individualized 0.5 cm and 1.0 cm bolus

STL files of boluses created in the program "Blender", were saved for the printing procedure, but before it were checked by using free software program "Meshmixer". The program "Meshmixer" is used to detect 3D objects defects, for example, an error in the scaling using a program "Blender". Likewise the "stair" artefacts, which means that an object is not smooth and on the surface it creates "stairs". In this case the program "Meshmixer" is used in order to smooth the surface [68].

3D models of boluses were printed (figure 35), following the process described in the previous (2^{nd}) step "3D printing of reconstructed patient (middle part of the face) from polylactic acid (PLA) material ***(was done by PhD student Antonio Jreije (KTU)),*** attaching/ fixing it to the surface of standard polymethyl methacrylate (PMMA) CT head phantom" (figure 29).

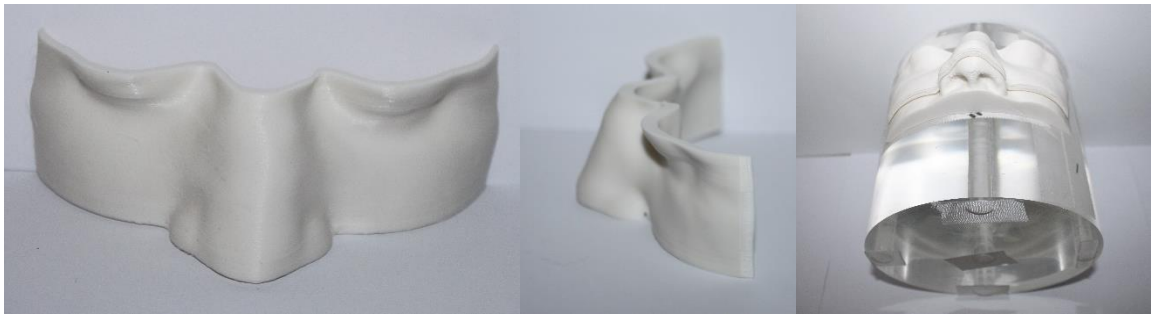

Fig 35. Printed bolus 0.5 cm bolus on the patient specific phantom

If the patient specific phantom was printed using polylactic acid (PLA) filament, with 90 % infill ratio, so 3D printed bolus with 100 % infill ratio. This caused higher HU value, even it is known and in a reference could be find (table 3) that HU value of the PLA is equal to 142, while 3D

printed patient specific phantom with 90 % infill ratio as already mentioned is equal to -32 HU. These data showed how important criteria infill ratio and 3D printing pattern is.

Table 3. HU values of PMMA and 3D printing material [70-72]

Material	**Hounsfield Unit**
PMMA	126 ±15 [70]
PLA	142 [71]
ABS	-54 ±13 [72]

2.2 Dosimetric evaluation of the data

In order to evaluate how 3D printed bolus fits to the patient specific phantom and evaluate the absorbed dose distribution, without and with bolus, depending on an air gaps (between bolus and patient specific phantom) and bolus thickness was used 3D treatment planning system “Eclipse” (figure 36). “Eclipse” is a treatment planning system (TPS) manufactured by Varian, that is designed for various types of treatments (3D-CRT, IMRT, VMAT, IGRT, also electron proton and brachytherapy treatments) [73].

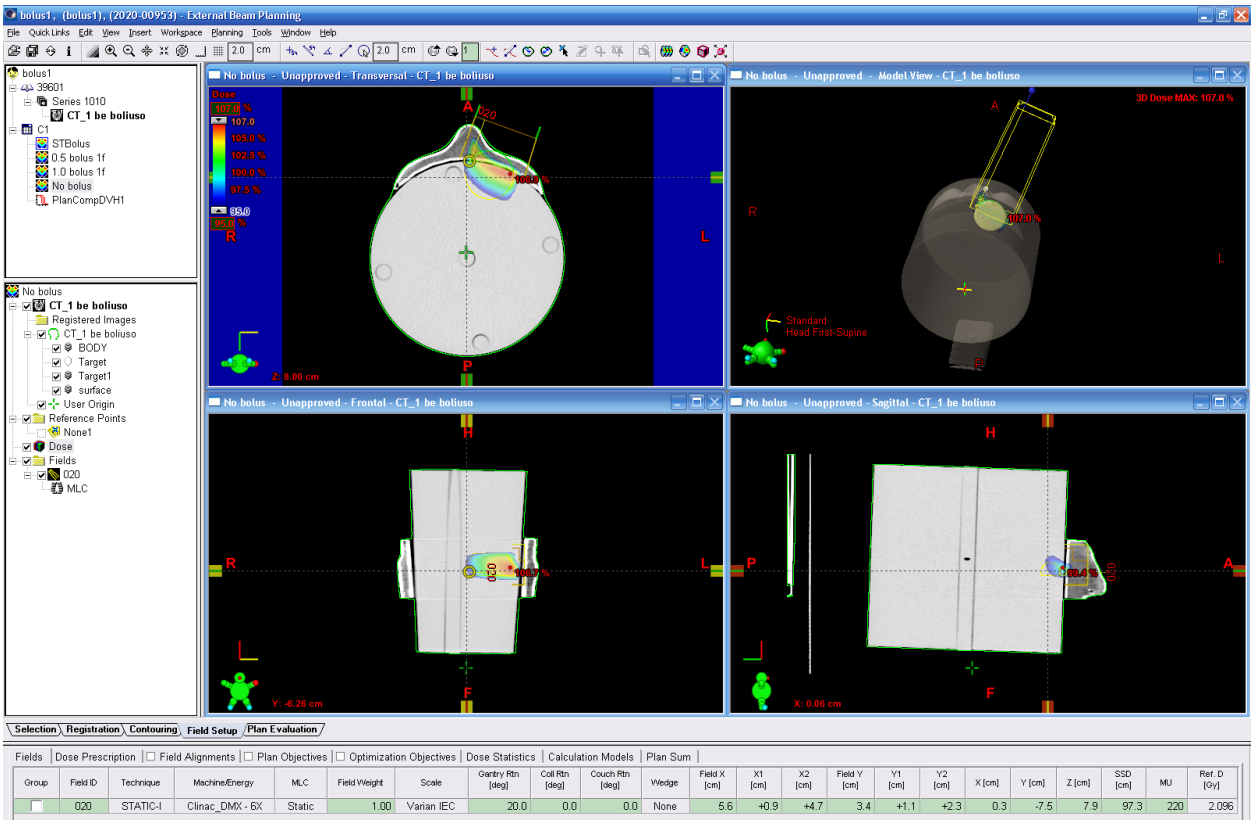

Fig 36. 3D treatment planning system “Eclipse” for the plan without bolus

The main workflow of dosimetric evaluation using 3D TPS consisted from two steps:

1. The first step was air gaps evaluation/ measurements between different thicknesses of the boluses. The air gaps under the 0.5 cm and 1.0 cm thickness 3D printed PLA individualized boluses were evaluated using 3D treatment planning system (TPS).

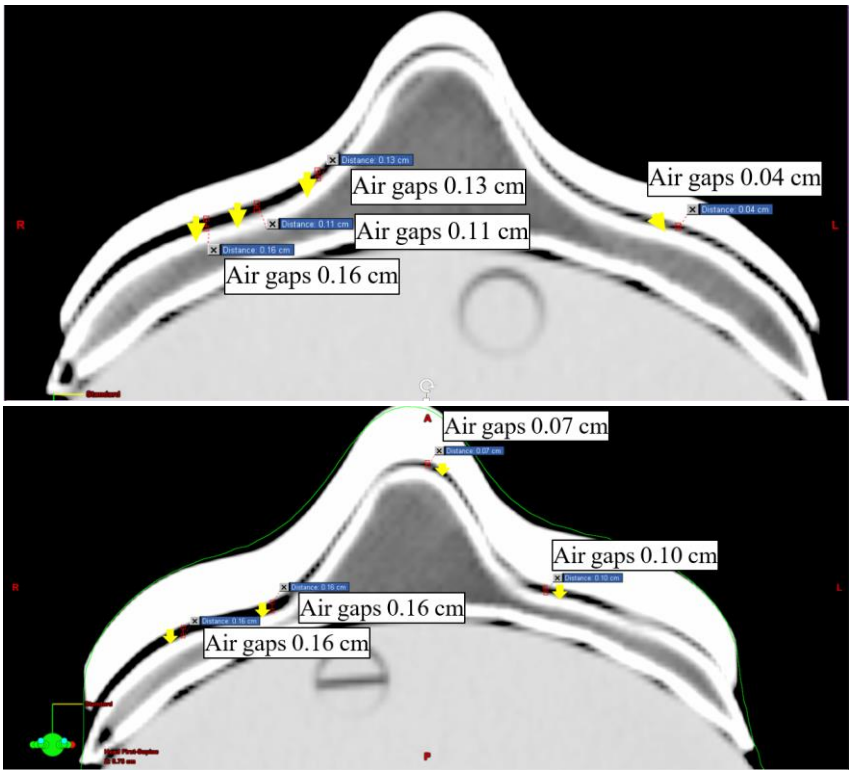

Fig 37. Marked air gaps between 0.5 cm thickness 3D printed PLA individualized bolus and the patient specific phantom. A – air gaps formed under the 0.5 cm bolus in a certain slice varied from 0.04 cm to 0.16 cm; B – air gaps created under the 1.0 cm bolus in a certain slice varied from 0.07 cm to 0.16 cm

Analysis of the air gaps formed in between was done slicing through the CT slices, measuring it in 2D slices (figure 37), determine where usually air gaps were formed. More data regarding to air gaps evaluations in different 2D slices are presented in an *Appendix 1*.

2. The second step creation of three single field treatment plans were planned for evaluation of the dose distribution without bolus and with individualized 3D PLA printed boluses (figure 34). Due to higher density of printed individualized boluses, was created so called additional structure converting high density HU (~469 HU) value to a lower density HU value (-30 HU), which imitates soft tissues (figure 38), as usually bolus is used to imitate (figure 39).

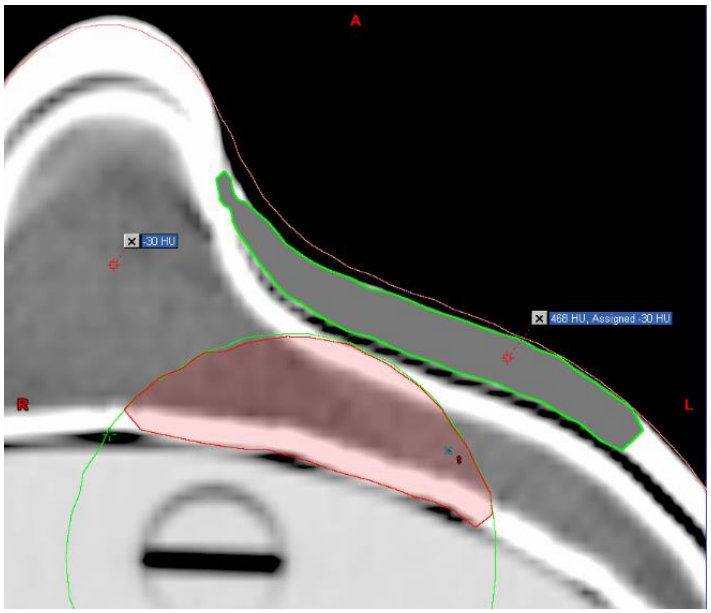

Fig 38. Additional structure on the 0.5 cm thickness bolus imitating soft tissue.

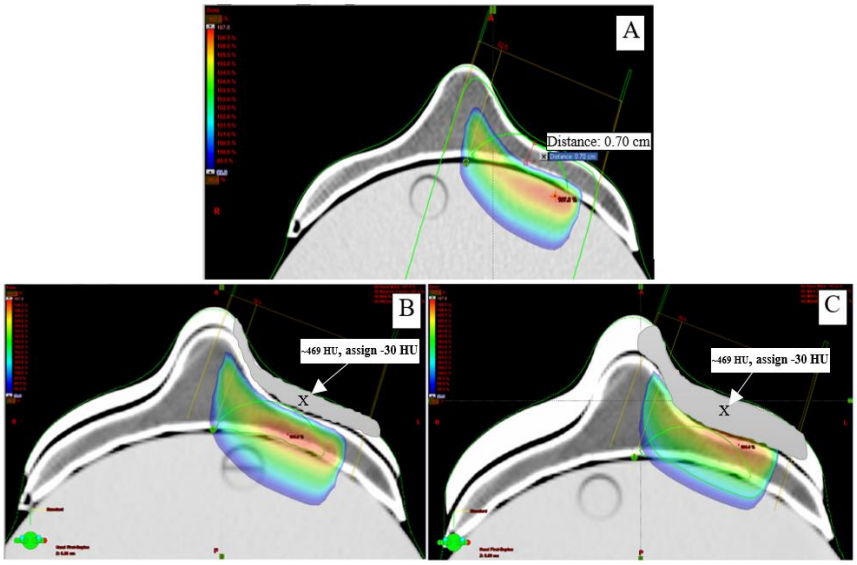

Fig 39. A - single field plan without bolus, B – single field plan with 0.5 cm thickness 3D printed PLA bolus, C- single field plan with 1 cm thickness 3D printed PLA bolus

As already mentioned, three single field plans with the same irradiation conditions have been created: field size 5.6 cm x 3.6 cm, gantry angle 20° (angle was chosen for the dose distribution evaluation from the left side of the patient specific phantom, because air gaps formed under the boluses were almost the same (symmetrically) distributed in both sides of the "patient" (figure 34 B and C)), irradiation energy 6 MeV energy, 2 Gy/fr. (table 4).

Table 4. Field size of the beam

Field X [cm]	X1 [cm]	X2 [cm]	Field Y [cm]	Y1 [cm]	Y2 [cm]
5.6	+0.9	+4.7	3.6	+1.2	+2.4

Surface dose was evaluated for the structure of 3.8 cm^3 volume, which has been cropped from the target (18 cm^3 volume) (figure 39).

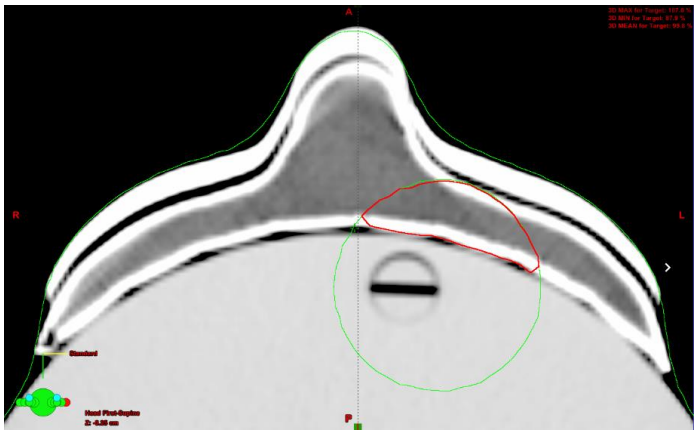

Fig 40. 3.8 cm^3 volume where the surface doses were evaluated

Whole plans data analysis were performed using dose volume histogram (DVH). DVH is a histogram showing relation from radiation dose to tissue volume (figure 40). It is one of the main tools evaluating treatment plan quality.

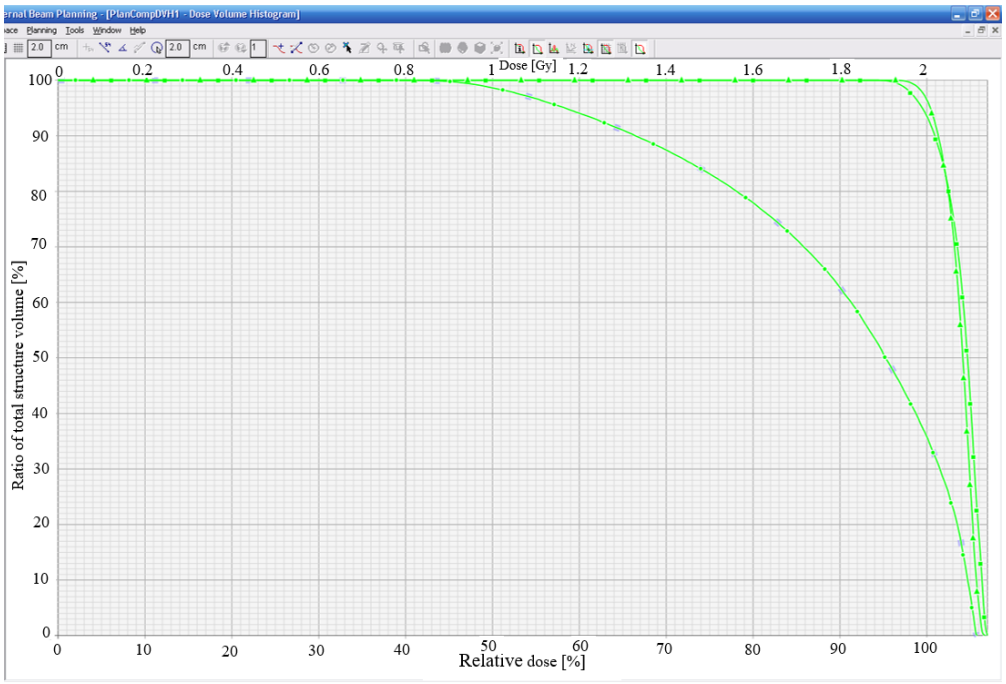

Fig 41. DVH for the single plan without bolus

3 Results

Radiotherapy aims to irradiate the tumor and save the surrounding healthy tissues as much as possible. High energy (MeV) photons create a skin-sparing effect, which is useful irradiating tumors located deep in a body [61], avoiding undesired early and late reactions of the skin. Therefore, the surface dose is vital due to normal tissue complication probability (NTCP), which might be the consequence of overexposure [74]. On the other hand, if the tumor is located near the surface, the skin-sparing effect reduces the absorbed dose to the target and the target will be underexposed [61]. In order to avoid that, a build-up boluses (additional body) are used, but the standard silicone bolus, even it is flexible, used on the irregular surfaces, like head and neck forms air gaps between bolus and patient, which results in inhomogeneity of the dose distribution. Therefore using customized 3D printed bolus minimizes uncertainties of the treatment procedure using high energy photons, created due to formed air gaps [1, 61]. Due to this reason, the main aim of this research was to determine the suitability of 3D printed boluses to a patient-specific phantom surface based on CT images (air gaps evaluation) and to compare 3 planned plans (one without bolus and two with different thickness boluses) efficiency for the treatment outcome.

Evaluation of the air gaps was done using the 3D treatment planning system "Eclipse", analyzing information seen in 2D slices and measuring the distance between bolus and patient-specific phantom (figure 41). In this way were analyzed two CT scanned experimental setups, using different thicknesses (0.5 cm and 1.0 cm) of individualized 3D printed PLA boluses on fabricated patient-specific head phantom (reconstructed from real patient CT scans).

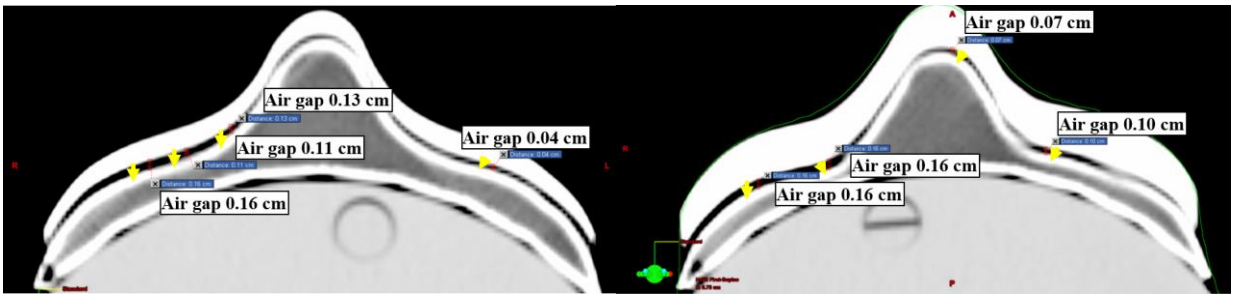

Fig 42. Marked air gaps between 0.5 cm and 1.0 cm thickness 3D printed PLA individualized bolus and the patient specific phantom. A – air gaps formed under the 0.5 cm bolus in a certain slice varied from 0.04 cm to 0.16 cm; B – air gaps created under the 1.0 cm bolus in a certain slice varied from 0.07 cm to 0.16 cm

Analysis of 2D slices for 0.5 cm and 1.0 cm individualized 3D printed PLA boluses showed, that air gaps formed almost symmetrically between bolus and patient-specific phantom (figure 41). The larger air gaps were formed in cheeks area (which varied from 0.4 mm to 2.1 mm for 0.5 cm bolus; while for 1.0 cm bolus it varied from 0.6 mm to 2.2 mm), while in nose region it differed from 0.7 mm to 1.3 mm (for 0.5 cm thickness bolus) and 1.4 mm maximum air gap was observed for 1.0 cm thickness bolus. According to G. Dipasquale et al. [75] air gaps formed between 3D printed bolus and skin were 1-2 mm. These results show good agreement to research project results, which

in studied 2D CT slices were 0.4-2.1 mm (0.5 bolus) and 0.7-2.2 (1.0 cm bolus). It is known, that using standard silicone bolus during head and neck irradiation with 6 MeV energy photons air gaps between bolus and patient usually could differ from 5 mm [2] to 10 mm [76]. The air gaps of 4 mm reduce the dose of approximately 4 % for basal layer, depending on field size and angle of incident, while air gaps of 10 mm, reduce the dose up to 10 % [2]. Therefore, it is significantly observed how air gaps could be minimized or even in some regions and avoided, using 3D printed boluses independently from the 3D printed bolus thickness.

Statistical analysis showed that averaged values of air gaps with 95% of the confidence interval for 0.5 cm thickness 3D printed PLA bolus is in the range of (0.14; 0.15) mm, for 1.0 cm thickness 3D printed PLA bolus with 95% of confidence interval it is (0.13; 0.15) mm, while Butson et. al reports that the mean ar gap observed under the 3D printed ABS bolus is 0.2 mm [2].

3D treatment plans analysis. Three single-field plans were created evaluating dose distribution for the surface volume (a surface part of the target). One of the plans was planned without a bolus, two others were planned with two different thicknesses boluses (0.5 cm and 1.0 cm), using the same planning parameters: field size 5.6 cm x 3.6 cm, gantry angle 20°, irradiation energy 6 MeV energy, 2 Gy/fr. It was observed, that in a single field plan planned without bolus (figure 38) the isodose was shifted inside the phantom/volume by the 0.70 cm (for 95 % coverage) and 1.00 cm (for 99 % coverage), that resulted in a lack of the dose on the surface.

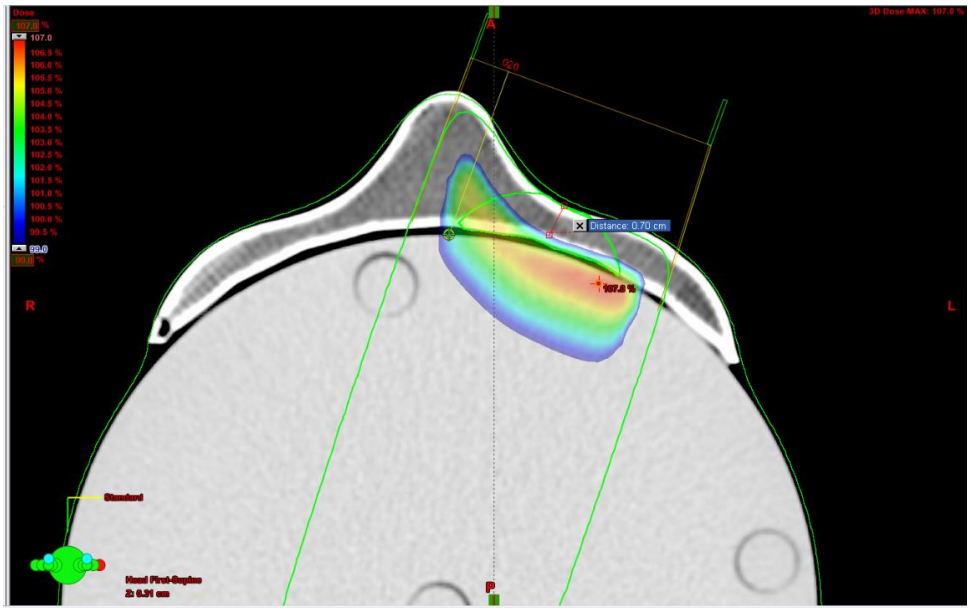

Fig 43. A single field plan without bolus

Also, analysing results of the plan, were used dose volume histograms (DVH) (figure 43), evaluating 95 %, 98 % and 99 % coverage of the surface volume. 95 % limit is usually used for 3D conformal radiotherapy treatment plans evaluation, but for irradiation head and neck cancer patients, then is used intensity modulated radiotherapy (IMRT) or volumetric arc therapy (VMAT)

techniques, due to theirs ability to ensure higher percentage of the target coverage, additionally are evaluated 98 % or/ and 99 % coverage [30]. Therefore, 95 % of the investigated surface volume was irradiated 57.64 % (1.15 Gy) from the prescribed 2 Gy per one fraction, while 98 % – surface volume was covered with 51.24 % (1.02 Gy), and 99 % – 47.96 % (0.96 Gy). It means, that without bolus the target will be underexposed and this will result a recurrence of the disease.

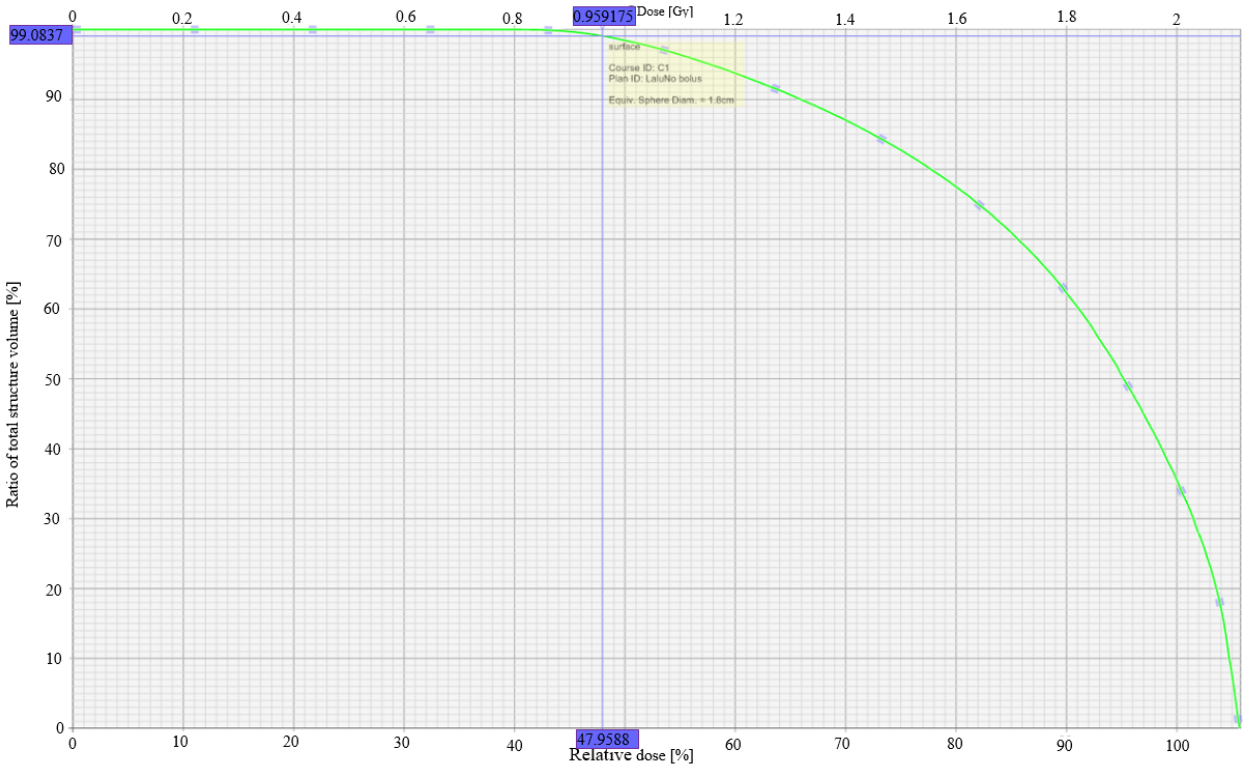

Fig 44. Dose volume histogram for the single plan without bolus

Two other plans using different thickness boluses showed significantly different results. The plan planned with 0.5 cm bolus (figure 44) showed, that 95 % of the same investigated surface volume was irradiated 99.5% (1.99 Gy) from the prescribed 2 Gy per one fraction, while 98 % – surface volume was covered with 98% (1.96 Gy), and 99 % – 97 % (1.94 Gy). Therefore, the data obtained from TPS has shown decrease of the surface volume dose planning “treatment” without bolus. Improvement of irradiation procedure imitating irradiation of the shallow target was done using different thickness (0.5 cm and 1.0 cm) individualized 3D printed PLA boluses was the next goal of this reasearch project.

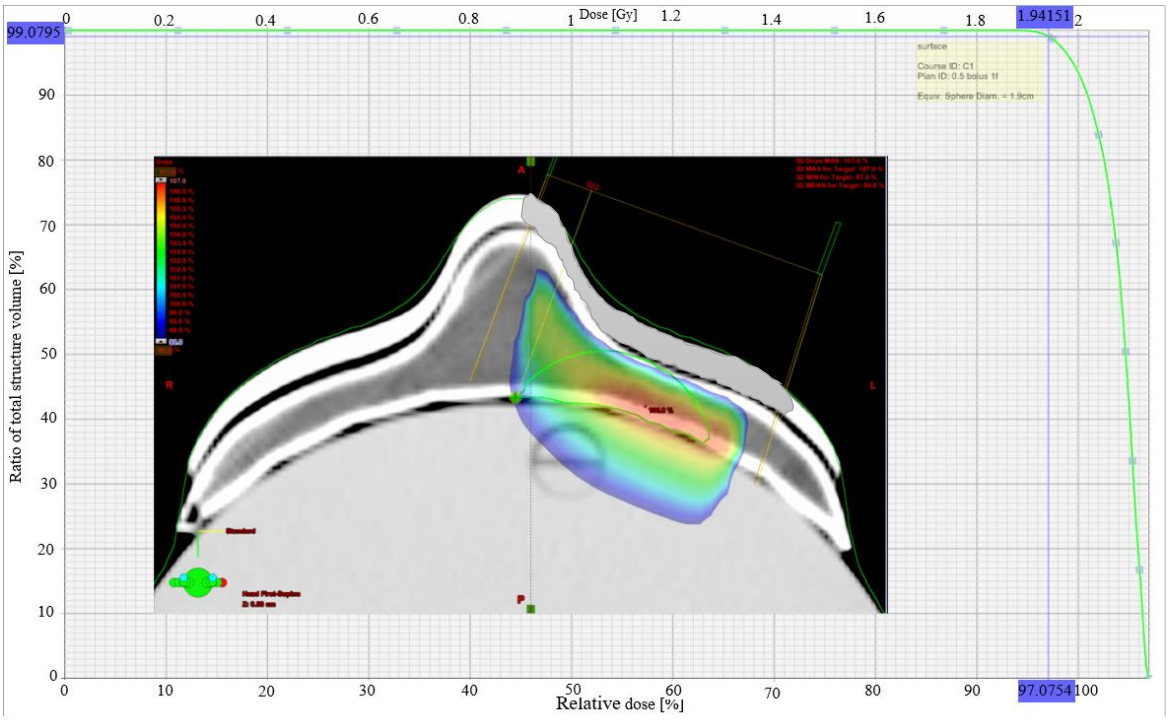

Fig 45. A single field plan with 0.5 cm thickness bolus and DVH of the plan

The same tendency was observed analysing plan with 1.0 cm bolus: 95 %: 100 % (2 Gy), 98 %: 99.5 % (1.99 Gy), and 99 % – 98.5 % (1.97 Gy) (figure 45).

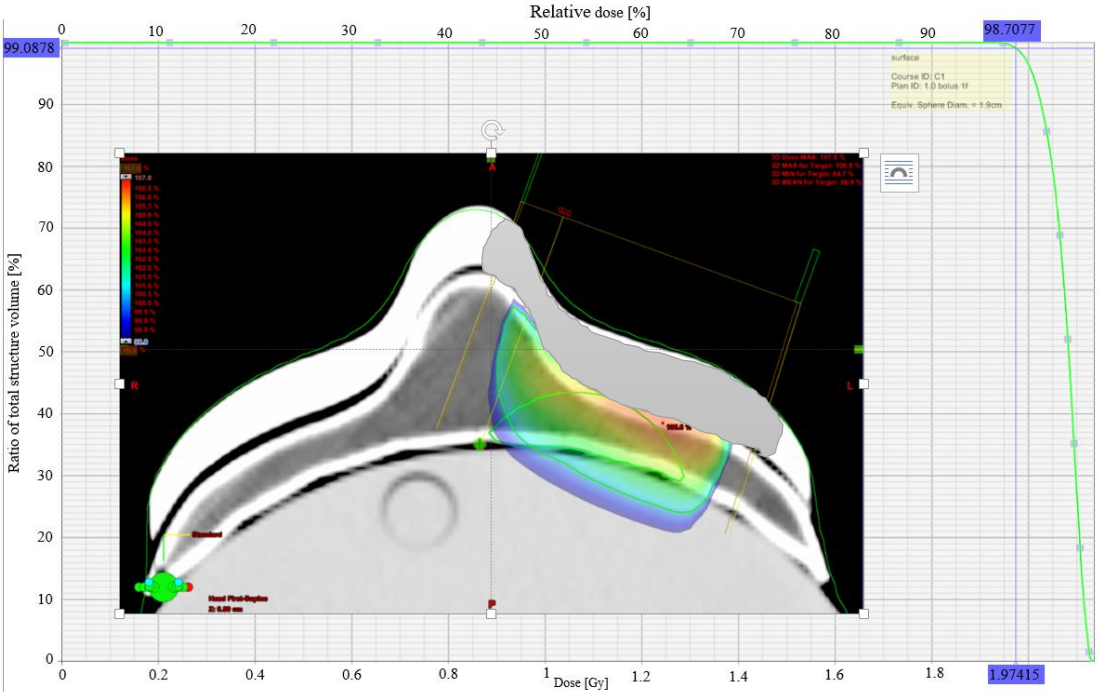

Fig 46. A single field plan with 1.0 cm thickness bolus and DVH of the plan

0.5 cm and 1.0 cm boluses results differ not so significantly (table 5 and figure 44, 45), so both thickness boluses could be successfully used in radiotherapy for head and neck shallow cancer irradiation.

Table 5. Doses at different volume (95%, 98%, 99% of structure volume)

A single field plan	**Doses with different volume (Gy)**		
	95%	**97%**	**99%**
Without bolus	1.15	1.02	0.96
With 0.5 cm bolus	1.99	1.96	1.94
With 1.0 cm bolus	2.00	1.99	1.97

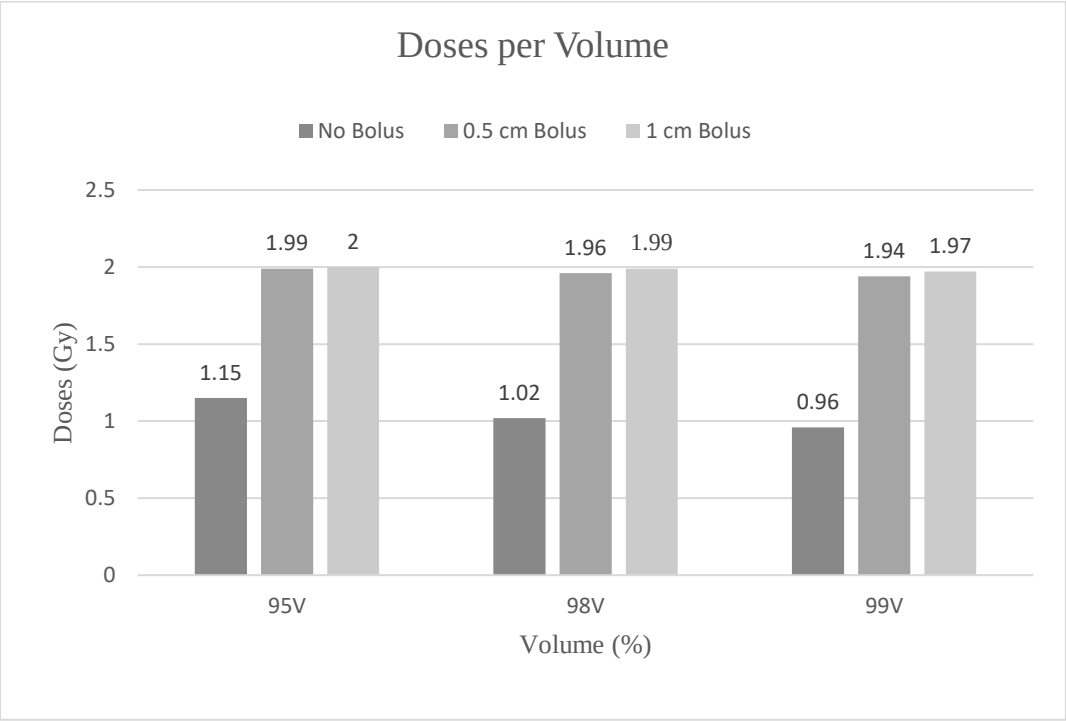

Fig 47. Histograms that shows absorbed dose calculations by TPS per volume of structure (95%, 98% and 99%) for the 3 single field plans: no bolus, 0.5 cm thickness bolus, 1.0 cm thickness bolus

These results using 0.5 cm and 1.0 cm individualized 3D printed PLA boluses could be comparable with other author's studies, where 3D printed boluses were used.

For example, according to Fujimoto K. et al. research compares the plans using 0.5cm thickness 3D printed ABS bolus with virtual bolus and commercial bolus [60], as well as, the additional study in comparison of different thickness boluses (0.5 cm, 1 cm, 2 cm and 3cm) plans were evaluated which showed that registered differences between calculated dose with the virtual boluses and a measured dose with different thickness bolus (0.5 cm, 1cm, 2 cm, 3 cm) is less than 1% at different depth (1 cm, 5 cm, 10 cm). In this study the thickness of air gaps registered reduced from 0.8 cm for commercially available silicone bolus to 0.2 cm between the 3D printed ABS bolus, this ensured efficient delivery of the dose to the target volume [61].

The surface volume irradiation dose with 0.5 cm and 1.0 cm boluses increased per 60%, 50% and 48% at 95%, 98% and 99% volumes in compare with a plan without bolus (table 5). Therefore, using individualized 0.5 cm thickness individualized 3D printed PLA bolus the dose difference from the prescribed dose 2Gy vary for different volume coverage (95%, 98%, 99%) (table 6). The calculated absorbed dose with treatment planning system (TPS) for 95% volume (95%V) coverage is 1.99 Gy, the difference (diff.) is 0.01 Gy (0.5%);. for 97%V coverage calculated dose is 1.97 Gy, diff. – 0.04 Gy (2%); for 99%V the calculated dose is 1.94, the diff. – 0.06 Gy (3%). Evaluation of 1 cm thickness bolus showed better results in 95%, 98 % and 99 % of structure volume coverage in compare with 0.5 cm bolus, but these results are not significant and difference varies from 0.5 % to 1.5 % (table 4). So the use of investigated 3D printed boluses are really promising and with some additional dosimetrical measurements could be successfully used in a clinical practice, especially for the concaved and uneven surfaces, like shallow head and neck cancer.

Table 6. Calculated difference between doses calculated by TPS and prescribed dose 2Gy

A single field plan	**Difference from prescribed dose 2Gy**					
	95%V		**97%V**		**99%V**	
	Gy	**%**	**Gy**	**%**	**Gy**	**%**
Without bolus	0.85	40.0	0.98	50.0	1.04	52.0
With 0.5 cm bolus	0.01	0.5	0.04	2.0	0.06	3.0
With 1.0 cm bolus	0.00	0.0	0.01	0.5	0.03	1.5

Three single field plans, one without bolus, 2 others with 0.5 cm and 1.0 cm thickness boluses, shows, how significant could be boluses, creating a build-up dose region for high energy photons (6 MeV) (figure 47).

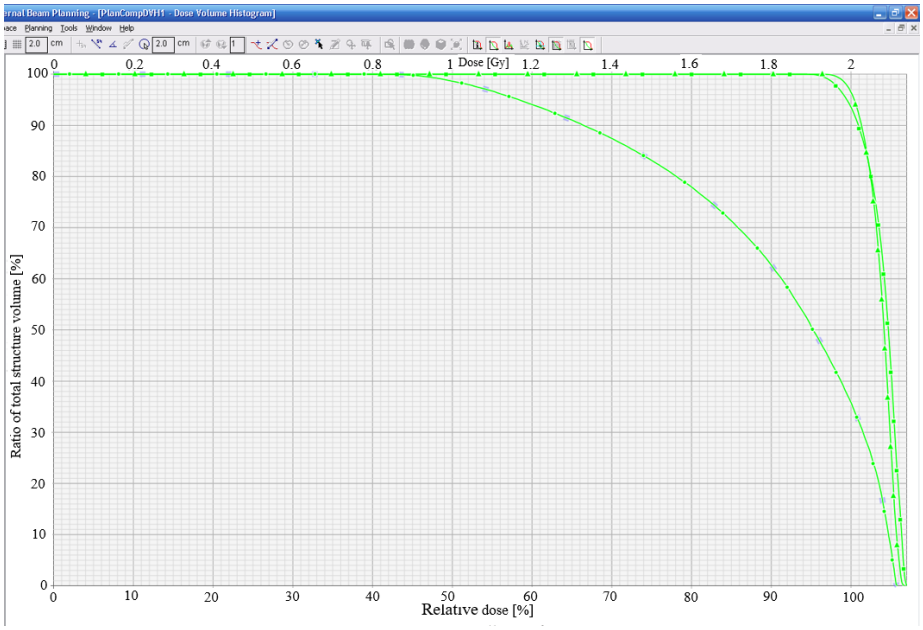

Fig 48. DVH for the three single field plans without bolus, with 1 cm and 0.5 cm thickness boluses

The second step analysis of the plans was done evaluating how determined air gaps are influencing isodose distribution. Isodose distribution evaluation presented shows that the build-up dose are clearly seen while using 0.5 cm and 1 cm thickness boluses (figure 48) during irradiation procedure. On the single field plan without bolus the isodose shift towards the deepr localizations are obrevable.

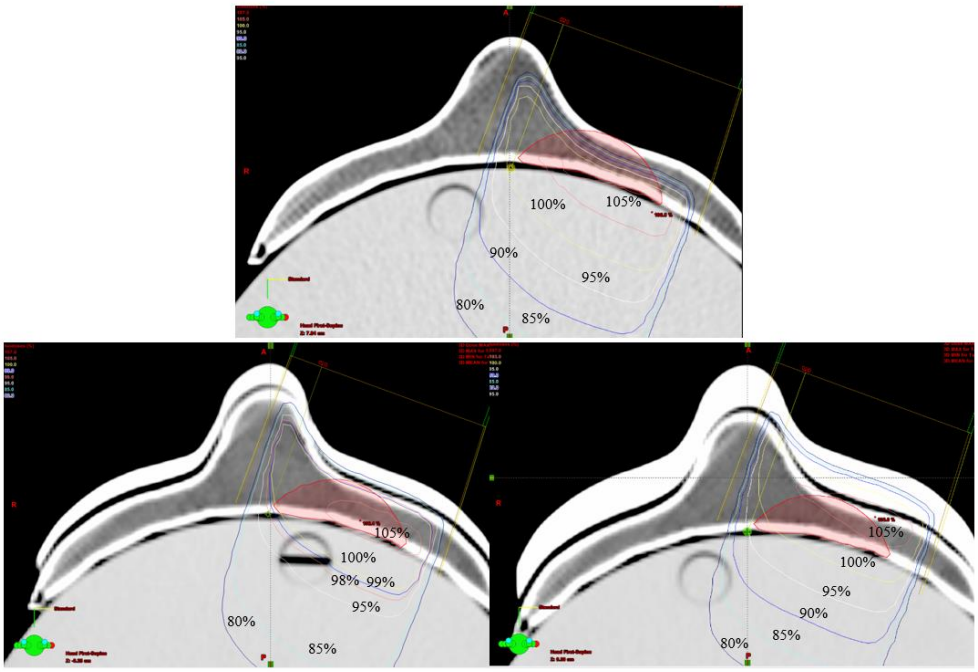

Fig 49. Isodose distribution at single field plan without bolus, with 0.5 cm and 1.0 cm thickness boluses

The isodose distribution for three single field plans are comperable to other studies as well (figure 49) [9]. While evaluation of isodose distribution of the single field plan with boluses (superflab and 3D printed flat) results in build up dose on the surface, while the skin sparing effect is absorvable on the dose distribution evaluation of a single field plan without bolus.

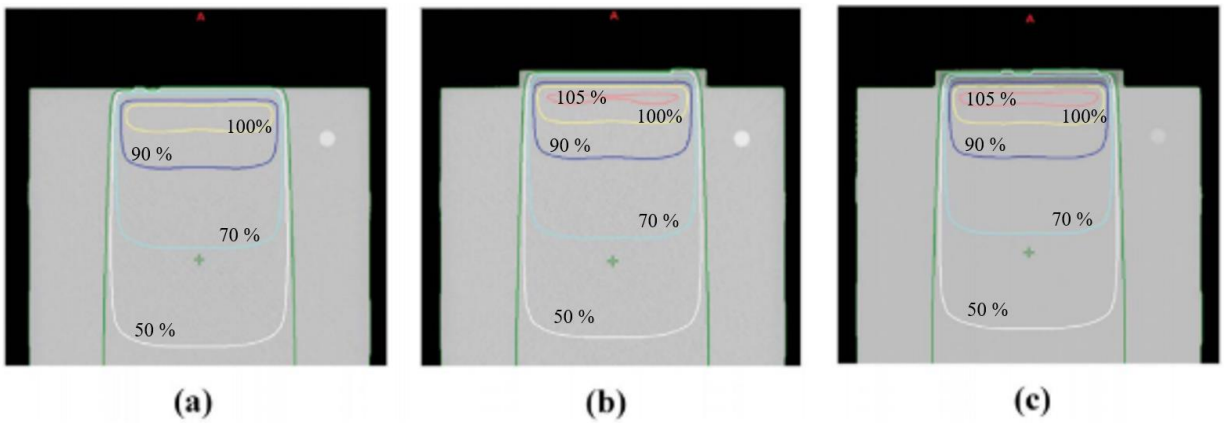

Fig 50. Dose distribution of the three treatment plans from the blue water phantom study [9]. A single plan without bolus (a), with superflab bolus (b) and with 3D printed flat bolus (c).

Therefore, analysis of the results using 3D printed PLA boluses showed, that using 3D printed bolus significantly increases the surface volume dose (more than ~40 %) while due to avoided or minimized air gaps (up to 2 mm) in compare with a standard silicone bolus influence for the isodose distribution is significant, evaluating possible “treatment” outcome for uneven shallow surfaces. The main issue for 3D printed bolus that it has to be soft tissue equivalent.

Conclusions

1. The absorbed dose measurements and isodose distribution evaluation were evaluated, using patient-specific phantom for the middle part of the face (eyes and nose region), imitating uneven surface and shallow head and neck cancer case irradiation procedure. It was found, that using tissue-equivalent polylactic acid (PLA) material with 90% infill ratio is possible to imitate soft tissues of the facial region where 3D printed HU value (-30 HU) showed a good agreement with soft tissues HU values on the head and neck region, which usually differs from -15 HU to -60 HU, while the reconstruction of different thickness (0.5 cm and 1.0 cm) individualized 3D printed PLA boluses showed, that with 100 % infill ratio showed, that it imitates more dense structures, like skull bone or upper jawbone (maxilla). Due to this reason for the dosimetric evaluation of the results using a 3D treatment planning system has to be created an additional structure of 3D printed bolus, imitating soft tissues with a lower HU value.

2. It was found, that air gaps formed between individualized 0.5 cm and 1.0 cm thickness 3D printed PLA boluses and patient-specific phantom differed from 0.4 mm to 2.1 mm for 0.5 cm thickness bolus, while for 1.0 cm thickness bolus it differed from 0.6 mm to 2.2 mm. Therefore, using individualized 3D printed boluses for uneven surface showed, that air gaps (up to 2 mm) could be minimized more than twice in comparison with a standard silicone bolus (formed air gaps usually differ up to 10 mm).

3. Single field treatment plans planned using the 3D treatment planning system “Eclipse” was used for the surface volume coverage and the isodose distribution evaluation without bolus and with bolus. It was found, that using 1.0 cm thickness was observed the best coverage of the surface volume, evaluating 95%, 98 % and 99 % (2.00 Gy, 1.99 Gy and 1.97 Gy) coverage from the maximum prescribed 2 Gy dose per one fraction, not so significant difference was also observed using 0.5 cm thickness bolus (1.99 Gy, 1.96 Gy, and 1.94 Gy respectively) while analysis and comparison without bolus showed more than 47 % difference from the prescribed 2 Gy dose/ fr. (1.20 Gy for 95 % volume coverage, 1.00 Gy (98 %) and 0.96 Gy (99 %)). Therefore, 0.5 cm and 1.0 cm thickness individualized 3D printed PLA boluses could be successfully used in clinical practice while irradiation without bolus means that the target will be underexposed and recurrence of the disease probability will increase.

AKNOWLEDGEMENTS

I would like to express my deepest appreciation and gratitude to my supervisor Lect. Dr. Jurgita Laurikaitiene. The completion of this work would not have been possible without her support and invaluable contribution throughout the duration of the writing and experiment performing process. Special thanks to her for patiently answering all my questions, sharing her unparalleled knowledge, and giving practical suggestions. There will never be enough words or works to appreciate her role in my study development. I am lucky to have her as my mentor, due to I had the honor to study from her and develop my efficiency in my field, as well as she showed how to be a good person, it was a pleasure to learn from her.

I would like to extend my sincere gratitude to the Medical Physics Ph.D. student Antonio Jreije, who gifted the most important – time, with his vulnerable help during printing phantom, and sharing his valuable experience in different modeling programs while modeling boluses. The 3D printed PLA phantom presented in this work is reconstructed with collaboration with Ph.D. Antonio Jreije, it was a pleasure for me to work with him.

I am extremely grateful for Benas Gabrielis Urbonavicius, who found a time to print a bolus during the country lockdown caused due to the novel COVID-19. As well as, I must mention his effort in answering the questions and ability to give the way to implement absorbed theoretical knowledge in practice. As one of his students, my greatest gratitude to his extensive knowledge and guidance.

I cannot begin to express my thanks to the head of the physics department Prof. Diana Adliene, who supports students. Despite her busy schedule she is always there to show her students the ways to improve their work, skills, and efficiency. Her invaluable advice, constructive advice, and patience cannot be underestimated.

I must mention Prof. Judita Puišo who was actively participating in the projects. Special thanks to her time and effort during my MSc. studies. I very much appreciate every invaluable advice and comments throughout my development process. Thanks for her questions which were helpful to improve the research on the wide range of scope. Finally, many thanks to the study center of whole physics departments in the Kaunas University of Technology for their guidance.

References

1. Kim, Shin-Wook & Shin, Hun-Joo & Kay, Chul Seung & Son, Seok Hyun. (2014). A Customized Bolus Produced Using a 3-Dimensional Printer for Radiotherapy. PloS one. 9. e110746. 10.1371/journal.pone.0110746.
2. BUTSON, M.J.; CHEUNG, T.; YU, P.; METCALFE, P. *Effects on skin dose from unwanted air gaps under bolus in photon beam radiotherapy.* Radiation Measurements, 2000. p. 201 - 204.
3. Didona A, Lancellotta V, Zucchetti C, et al. Is volumetric modulated arc therapy with constant dose rate a valid option in radiation therapy for head and neck cancer patients?. *Rep Pract Oncol Radiother*. 2018;23(3):175–182. doi:10.1016/j.rpor.2018.02.007
4. Puri DR, Chou W, Lee N. Intensity-modulated radiation therapy in head and neck cancers: dosimetric advantages and update of clinical results. *Am J Clin Oncol*. 2005;28(4):415–423. doi:10.1097/01.coc.0000162443.08446.00
5. Martini, S., Arcadipane, F., Franco, P., Iorio, G. C., Bartoncini, S., Gallio, E., Guarneri, A. S., & Ricardi, U. (2020). Radiation therapy for oligometastatic oropharyngeal cancer. *BJR case reports*, *6*(1), 20190021. https://doi.org/10.1259/bjrcr.20190021
6. Mokhtar Maha, Ehab M.Attalla, Nashaat A. Deiab, Ahmed Soltan, H. Abou-Shady, Amr Amin. ((Nov. - Dec. 2015). Comparative dosimetry of forward and inverse treatment planning for Intensity- Modulated Radiotherapy of prostate cancer. *IOSR Journal of Applied Physics (IOSR-JAP)*, 97-106.
7. Radiotherapy in the management of orbital lymphoma. *Int J Radiat Oncol Biol Phys*. 1999;44(1):31–36. doi:10.1016/s0360-3016(98)00535-5
8. Dosimetric, Radiobiological and Secondary Cancer Risk Evaluation in Head-and-Neck Three-dimensional Conformal Radiation Therapy, Intensity-Modulated Radiation Therapy, and Volumetric Modulated Arc Therapy: A Phantom Study. Rehman JU1,Isa M2,Ahmad N1,Nasar G3,Asghar HMNUHK1,Gilani ZA1,Chow JCL2,Afzal M4,Ibbott GS5. Journal of Medical Physics / Association of Medical Physicists of India, 01 Apr 2018, 43(2):129-135
9. Zhang, S., Yang, R., Shi, C., Li, J., Zhuang, H., Tian, S., & Wang, J. (2019). Noncoplanar VMAT for Brain Metastases: A Plan Quality and Delivery Efficiency Comparison With Coplanar VMAT, IMRT, and CyberKnife. *Technology in cancer research & treatment*, *18*, 1533033819871621. https://doi.org/10.1177/1533033819871621
10. International Commission on Radiation Units and Measurements 2006 ICRU Report 76Measurement Quality Assurance for Ionizing Radiation Dosimetry Bethesda, Maryland, International Commission on Radiation Units and Measurements
11. Hogstrom et al. 1981; Schoknechtand Khatib 1982; Mackie et al. 1985; Mohan et al. 1986; Bortfeld et al. 1993
12. Mackieet al. 1985; Mohan et al. 1986; Ahnesjö et al. 1987; Mackie et al. 1988; Ahnesjö 1989; Scholz et al. 2003b

13. Akino Y, Das IJ, Bartlett GK, Zhang H, Thompson E, Zook JE. Evaluation of superficial dosimetry between treatment planning system and measurement for several breast cancer treatment techniques. *Med Phys*. 2013;40(1):011714. doi:10.1118/1.4770285
14. Wang L, Cmelak AJ, Ding GX. A simple technique to improve calculated skin dose accuracy in a commercial treatment planning system. J Appl Clin Med Phys. 2018;19:191-197.
15. CHARLES MAYO, MARY K. MARTEL, LAWRENCE B. MARKS, JOHN FLICKINGER, JIHO NAM, AND JOHN KIRKPATRICK. Radiation dose – volume effects of optic nerves and chiasm. *Elsevier, Int. J. Radiation Oncology Biol. Phys*., Vol. 76, No. 3, 2010.
16. Carrara M., Fallai C., Gambarini G., et al. Fricke gel-layer dosimetry in high dose-rate brachytherapy. Applied Radiation and Isotopes, 68 (2010). p. 722–725.
17. BALDOCK, C.; DE DEENE Y.; DORAN, S.; IBBOTT, G.; JIRASEK, A.; LEPAGE, M.; MCAULEY, K. B.; OLDHAM, M.; SCHREINER, L.J. *Polymer Gel dosimetry.* Institute of Physics and Engineering in Medicine, 2010.
18. Miglė Staliulionytė INVESTIGATION OF PROPERTIES OF RADIOSENSITIVE HYDROGELS Master's Final Degree Project Supervisor Doc. dr. Judita Puišo KAUNAS, 2018
19. Chaikh, Abdulhamid & Gaudu, Arnaud & Balosso, Jacques. (2014). Monitoring methods for skin dose in interventional radiology. International Journalof Cancer Therapy and Oncology. 3. 03011. 10.14319/ijcto.0301.1
20. Podgorsak, Ervin B. (2010). *Radiation physics for medical physicists* (2nd, enl. ed., Biological and medical physics, biomedical engineering). Heidelberg: Springer.
21. Cakmak, Emine & Tuncel, Nina & sındır, Bora. (2015). Assessment of Organ Dose by Direct and Indirect Measurements for a Wide Bore X-Ray Computed Tomography Unit That Used in Radiotherapy *. International Journal of Medical Physics, Clinical Engineering and Radiation Oncology. 4. 132-142. 10.4236/ijmpcero.2015.42017.
22. LOWE, D. Thermoluminescence: Dosimetry and applications. In Nuclear Instruments and Methods [interactive]. 1980. Vol. 176, no. 3, p. 628. Access through internet: <http://linkinghub.elsevier.com/retrieve/pii/0029554X80904048>.
23. YAHYAABADI, A. et al. CHARACTERISTICS OF THERMOLUMINESCENCE LiF : Mg , Cu , Ag NANOPHOSPHOR. In . 2018. no. April, p. 1–7
24. YOSHIMURA, E.M. et al. Characterization and performance tests of a new osl / tl personal dosemeter for individual use. In . 2018. no. April, p. 1–8
25. MAIA, A.F. - CALDAS, L.V.E. Response of TL materials to diagnostic radiology X radiation beams. In Applied Radiation and Isotopes . 2010. Vol. 68, no. 4, p. 780–783.
26. SHARMA, K. et al. BaSO 4 :Eu as an energy independent thermoluminescent radiation dosimeter for gamma rays and C 6+ ion beam. In Radiation Physics and Chemistry [interactive]. 2018. Vol. 145, p. 64–73. [looked at 2018-05-07]. . Access through internet: <http://linkinghub.elsevier.com/retrieve/pii/S0969806X17306746>.
27. FERNÁNDEZ, S et al. Thermoluminescent dosimeters for low dose X-ray measurements. In

Applied Radiation and Isotopes [interactive]. 2016. Vol. 107, p. 340–345. [looked at 2018-05-07]. Access through internet: <https://www.sciencedirect.com/science/article/pii/S0969804315302487>.

28. Thermoluminescence dosimetry and its applications in medicine--Part 1: Physics, materials and equipment. In [interactive]. 1995. [looked at 2018-05-06]. . Access through internet: <https://www.researchgate.net/publication/15326128>.
29. AZORÍN N., J. Thermoluminescence Dosimetry (TLD) and its Application in Medical Physics. In AIP Conference Proceedings [interactive]. 2004. Vol. 724, no. 2004, p. 20–27. Access through internet: <http://aip.scitation.org/doi/abs/10.1063/1.1811814>.
30. Palmans H, Andreo P, Huq MS, Seuntjens J, Christaki KE, Meghzifene A. Dosimetry of small static fields used in external photon beam radiotherapy: Summary of TRS-483, the IAEA-AAPM international Code of Practice for reference and relative dose determination. *Med Phys*. 2018;45(11):e1123–e1145. doi:10.1002/mp.13208
31. Alan E. Nahum. C it Th avity Theory, Stopping-Power Ratios. AAPM Summer School, CLINICAL DOSIMETRY FOR RADIOTHERAPY, 21-25 June 2009, Colorado College, Colorado Springs, USA. https://www.aapm.org/meetings/09SS/documents/03Nahum-CavityTheorywithCorrections.pdf
32. https://oncologymedicalphysics.com/radiation-detectors/#radiation-detectors-cavity-theory
33. Kamil, M Ubaidullah & Shakeel-ur-Rahman, Dr. (2013). Medical Facilities at KIRAN, Karachi.
34. Filippou, V., & Tsoumpas, C. (2018). Recent advances on the development of phantoms using 3D printing for imaging with CT, MRI, PET, SPECT, and ultrasound. *Medical physics*, *45*(9), e740–e760. Advance online publication. https://doi.org/10.1002/mp.13058
35. Antonovic, Laura & Gustafsson, Håkan & Carlsson, Gudrun & Carlsson Tedgren, Asa. (2009). Evaluation of a lithium formate EPR dosimetry system for dose measurements around (192)Ir brachytherapy sources. Medical physics. 36. 2236-47. 10.1118/1.3110068.
36. Mutic, Sasa & Palta, Jatinder & Butker, Elizabeth & Das, Indra & Huq, M. Saiful & Loo, Leh-Nien & Salter, Bill & McCollough, Cynthia & Van Dyk, Jacob. (2003). Quality assurance for computed-tomography simulators and the computed-tomography-simulation process: Report of the AAPM Radiation Therapy Committee Task Group No. 66. Medical physics. 30. 2762-92. 10.1118/1.1609271.
37. Wildgruber, M., Müller-Wille, R., Goessmann, H., Uller, W., & Wohlgemuth, W. A. (2016). Direct Effective Dose Calculations in Pediatric Fluoroscopy-Guided Abdominal Interventions with Rando-Alderson Phantoms - Optimization of Preset Parameter Settings. *PloS one*, *11*(8), e0161806. https://doi.org/10.1371/journal.pone.0161806
38. Santos, Adriano & Vieira, J.W.. (2009). 'Voxelization' of Alderson-Rando phantom for use in numerical dose measuring. Cellular and molecular biology (Noisy-le-Grand, France). 55. 7-12. 10.1170/T867.
39. Yea, J. W., Park, J. W., Kim, S. K., Kim, D. Y., Kim, J. G., Seo, C. Y., Jeong, W. H., Jeong,

M. Y., & Oh, S. A. (2017). Feasibility of a 3D-printed anthropomorphic patient-specific head phantom for patient-specific quality assurance of intensity-modulated radiotherapy. *PloS one*, *12*(7), e0181560. https://doi.org/10.1371/journal.pone.0181560

40. Hazelaar, C., van Eijnatten, M., Dahele, M., Wolff, J., Forouzanfar, T., Slotman, B. and Verbakel, W.F. (2018), Using 3D printing techniques to create an anthropomorphic thorax phantom for medical imaging purposes. Med. Phys., 45: 92-100. doi:10.1002/mp.12644
41. Yea JW, Park JW, Kim SK, Kim DY, Kim JG, et al. (2017) Feasibility of a 3D-printed anthropomorphic patient-specific head phantom for patient-specific quality assurance of intensity-modulated radiotherapy. PLOS ONE 12(7): e0181560. https://doi.org/10.1371/journal.pone.0181560
42. Petersen C, Würschmidt F. Late Toxicity of Radiotherapy: A Problem or a Challenge for the Radiation Oncologist? Breast Care (Basel). 2011 Oct;6(5):369-374. doi: 10.1159/000334220. Epub 2011 Oct 31. PMID: 22619647; PMCID: PMC3357174
43. INTERNATIONAL ATOMIC ENERGY AGENCY. *Radiotherapy in cancer care: facing the global challenge.* Vienna: 2017.
44. INTERNATIONAL ATOMIC ENERGY AGENCY. *Radiation oncology physics: A handbook for teachers and students*. Vienna: 2005.
45. Parker, W., & Patrocinio, H. (2005). Chapter 7 : Clinical Treatment Planning in External Photon Beam Radiotherapy.
46. Lee, M. Y., Han, B., Jenkins, C., Xing, L., & Suh, T. S. (2016). A depth-sensing technique on 3D-printed compensator for total body irradiation patient measurement and treatment planning. *Medical physics*, *43*(11), 6137. https://doi.org/10.1118/1.4964452.
47. Khan F.M., Gibbson J.P. The Physics of Radiation Therapy. Fifth edition, Wolters Kluwer, 2014
48. Constantinou C, Harrington JC. Tissue compensators made of solid water or lead for megavoltage X-ray radiotherapy. *Med Dosim*. 1989;14(1):41–47. doi:10.1016/0958-3947(89)90137-4.
49. Keshelava Lali, Andrejaitis Artūras, Čerapaitė-Trušinskienė Reda, Dimitrova Todorka, & Laurikaitienė, Jurgita. (2019). 3D printed boluses usage in radiotherapy. Medical Physics in the Baltic States: Proceedings of the 14th International Conference on Medical Physics, Kaunas, Lithuania, 7-9 November, 2019, 125-128.
50. So-Yeon Park, Chang Heon Choi, Jong Min Park, MinSoo Chun, Ji Hye Han, Jung-in Kim- A Patient-Specific Polylactic Acid Bolus Made by a 3D Printer for Breast Cancer Radiation Therapy.
51. Sroka M., Regula J., Lobodziec W.The influence of the bolus-surface distance on the dose distribution in the build-up region. (2010) Reports of Practical Oncology and Radiotherapy, 15 (6) , pp. 161-164.
52. Rong Y1, Yadav P, Welsh JS, Fahner T, Paliwal B. Med Dosim. 2012 Autumn;37(3):233-9. doi: 10.1016/j.meddos.2011.09.001. Epub 2012 Feb 24. Postmastectomy radiotherapy with

integrated scar boost using helical tomotherapy

53. FISCHBACH, M.; HÄLG, R.A.; HARTMANN, M.; BESSERER,J.; GRUBER,G.; SCHNEIDER, U. *Measurement of skin and target dose in post – mastectomy radiotherapy using 4 and 6 MV photon beams*. Radiation Oncology, 2013.
54. Zoljalali Moghaddam, S., Baghani, H., Mahdavi, S. (2018). Evaluating the performance of a 3D PLA buildup bolus in breast intraoperative radiotherapy.. *Iranian Journal of Medical Physics*, 15(Special Issue-12th. Iranian Congress of Medical Physics), 358-358. doi: 10.22038/ijmp.2018.13022
55. Chiu, T., Tan, J., Brenner, M., Gu, X., Yang, M., Westover, K., Strom, T., Sher, D., Jiang, S., Zhao, B., 2018. Three-dimensional printer-aided casting of soft, custom silicone boluses (SCSBs) for head and neck radiation therapy. Pract. Radiat. Oncol. 8, e167–e174. https://doi.org/10.1016/j.prro.2017.11.001.
56. Laurikaitienė, J., Tzirkalov, T., Dimitrova, T.L., Laurikaitis, M. Evaluation of skin dose under the bolus for post-operative breast cancer treatment. Medical physics in the Baltic States: proceedings of the 13th international conference on medical physics, Kaunas, Lithuania, 9-11 November, 2017. Kaunas: Kaunas University of Technology. ISSN 1822-5721. 2017, p. 69-72.
57. Park JW, Yea JW. Three-dimensional customized bolus for intensity-modulated radiotherapy in a patient with Kimura's disease involving the auricle.
58. Tino, R., Yeo, A., Leary, M., Brandt, M., & Kron, T. (2019). A Systematic Review on 3D-Printed Imaging and Dosimetry Phantoms in Radiation Therapy. *Technology in cancer research & treatment*, *18*, 1533033819870208. https://doi.org/10.1177/1533033819870208
59. Razi, T., Niknami, M., & Alavi Ghazani, F. (2014). Relationship between Hounsfield Unit in CT Scan and Gray Scale in CBCT. *Journal of dental research, dental clinics, dental prospects*, *8*(2), 107–110. https://doi.org/10.5681/joddd.2014.019
60. Broder J, Preston R. Imaging the head and brain. In: Broder J, ed. Diagnostic Imaging for the Emergency Physician. Philadelphia, PA: Elsevier Saunders; 2011: 1-45
61. Efficacy of patient-specific bolus created using three-dimensional printing technique in photon radiotherapy Fujimoto K., Shiinoki T., Yuasa Y., Hanazawa H., Shibuya K. (2017) Physica Medica, 38 , pp. 1-9.
62. Chiu, T., Tan, J., Brenner, M., Gu, X., Yang, M., Westover, K., Strom, T., Sher, D., Jiang, S., Zhao, B., 2018. Three-dimensional printer-aided casting of soft, custom silicone boluses (SCSBs) for head and neck radiation therapy. Pract. Radiat. Oncol. 8, e167–e174. https://doi.org/10.1016/j.prro.2017.11.001
63. Kumar, R., Sharma, S. D., Deshpande, S., Ghadi, Y., Shaiju, V. S., Amols, H. I., & Mayya, Y. S. (2009). Acrylonitrile Butadiene Styrene (ABS) plastic based low cost tissue equivalent phantom for verification dosimetry in IMRT. *Journal of applied clinical medical physics*, *11*(1), 3030. https://doi.org/10.1120/jacmp.v11i1.3030
64. Aimar, A., Palermo, A., & Innocenti, B. (2019). The Role of 3D Printing in Medical

Applications: A State of the Art. *Journal of healthcare engineering*, *2019*, 5340616. https://doi.org/10.1155/2019/5340616

65. Sarah Burleson, Jamie Baker, An Ting Hsia, Zhigang Xu. Use of 3D printerd to create a patient-specific 3D bolus for external beam therapy. 2015.
66. Huang, J., Chen, S.J., Xue, Z., Withayachumnankul, W., & Fumeaux, C. (2018). Impact of Infill Pattern on 3D Printed Dielectric Resonator Antennas. *2018 IEEE Asia-Pacific Conference on Antennas and Propagation (APCAP)*, 233-235.
67. Ricotti R, Ciardo D, Pansini F, et al. Dosimetric characterization of 3D printed bolus at different infill percentage for external photon beam radiotherapy. *Phys Med*. 2017;39:25–32. doi:10.1016/j.ejmp.2017.06.004
68. Ricotti R, Ciardo D, Pansini F, et al. Dosimetric characterization of 3D printed bolus at different infill percentage for external photon beam radiotherapy. *Phys Med*. 2017;39:25–32. doi:10.1016/j.ejmp.2017.06.004
69. Zhao, Yizhou & Moran, Kathryn & Yewondwossen, Mammo & Allan, James & Clarke, Scott & Rajaraman, Murali & Wilke, Derek & Joseph, Paul & Robar, James. (2017). Clinical applications of 3-dimensional printing in radiation therapy. Medical Dosimetry. 42. 10.1016/j.meddos.2017.03.001.
70. Gear JI, Cummings C, Craig AJ, et al. Abdo-Man: a 3D-printed anthropomorphic phantom for validating quantitative SIRT. EJNMMI Phys. 2016;3:17–32. [PMC free article] [PubMed] [Google Scholar]
71. Tran-Gia J, Schlogl S, Lassmann M. Design and fabrication of kidney phantoms for internal radiation dosimetry using 3D printing technology. J Nucl Med. 2016;57:1998–2005. [PubMed] [Google Scholar]
72. Robinson AP, Tipping J, Cullen DM, et al. Organ-specific SPECT activity calibration using 3D printed phantoms for molecular radiotherapy dosimetry. EJNMMI Phys. 2016;3:12–22. [PMC free article] [PubMed] [Google Scholar]
73. Zhang, Y., Le, A.H., Tian, Z., Iqbal, Z., Chiu, T., Gu, X., Pugachev, A., Reynolds, R., Park, Y.K., Lin, M.-H. and Stojadinovic, S. (2019), Modeling Elekta VersaHD using the Varian Eclipse treatment planning system for photon beams: A single-institution experience. J Appl Clin Med Phys, 20: 33-42. doi:10.1002/acm2.12709
74. Akbas, Ugur & Kesen, Nazmiye & Koksal, Canan & Bilge, Hatice. (2016). Surface and Buildup Region Dose Measurements with Markus Parallel-Plate Ionization Chamber, GafChromic EBT3 Film, and MOSFET Detector for High-Energy Photon Beams. Advances in High Energy Physics. 2016. 10.1155/2016/8361028.
75. Improving 3D-printing of megavoltage X-rays radiotherapy bolus with surface-scanner Giovanna Dipasquale, Alexis Poirier, Yannick Sprunger, Johannes Wilhelmus Edmond Uiterwijk & Raymond Miralbell Radiation Oncology volume 13, Article number: 203 (2018)

76. Khan Y, Villarreal-Barajas JE, Udowicz M, Sinha R, Muhammad W, et al. (2013) Clinical and dosimetric implications of air gaps between bolus and skin surface during radiation therapy. J Cancer Ther 4: 1251–1255.

Appendices

Appendix 1 – air gaps between the individualized 3D printed PLA phantom and bolus.

Air gaps formed under the bolus decreases the surface dose respectively. The larger the air gaps, the less the absorbed dose on the surface is.

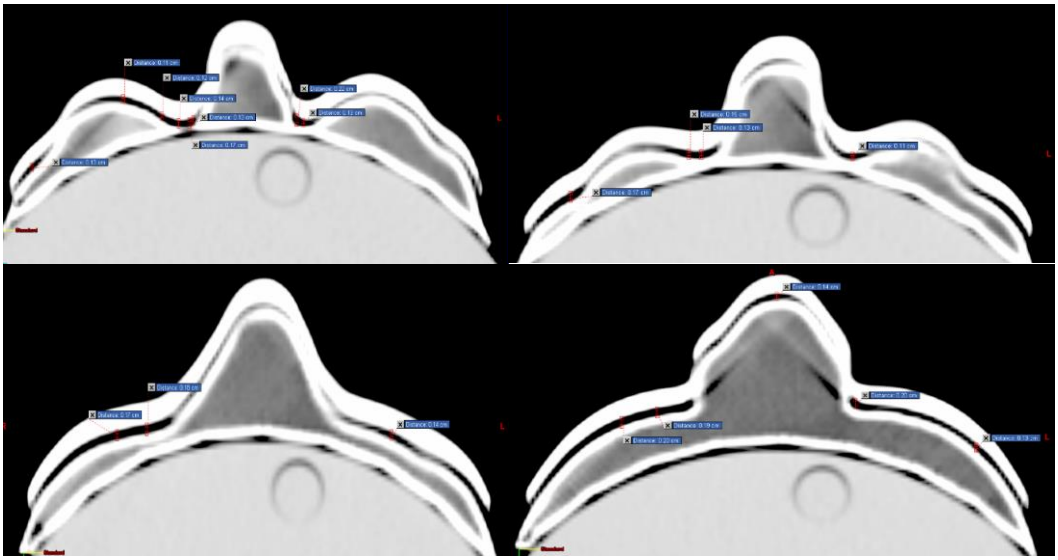

Fig 51. Air gaps formed below the 0.5 cm thickness 3D printed PLA bolus.

Marked air gaps between 1 cm thickness bolus 3D printed PLA individualized bolus and on the patient-specific 3D printed PLA phantom, which is placed on the CT head PMMA phantom.

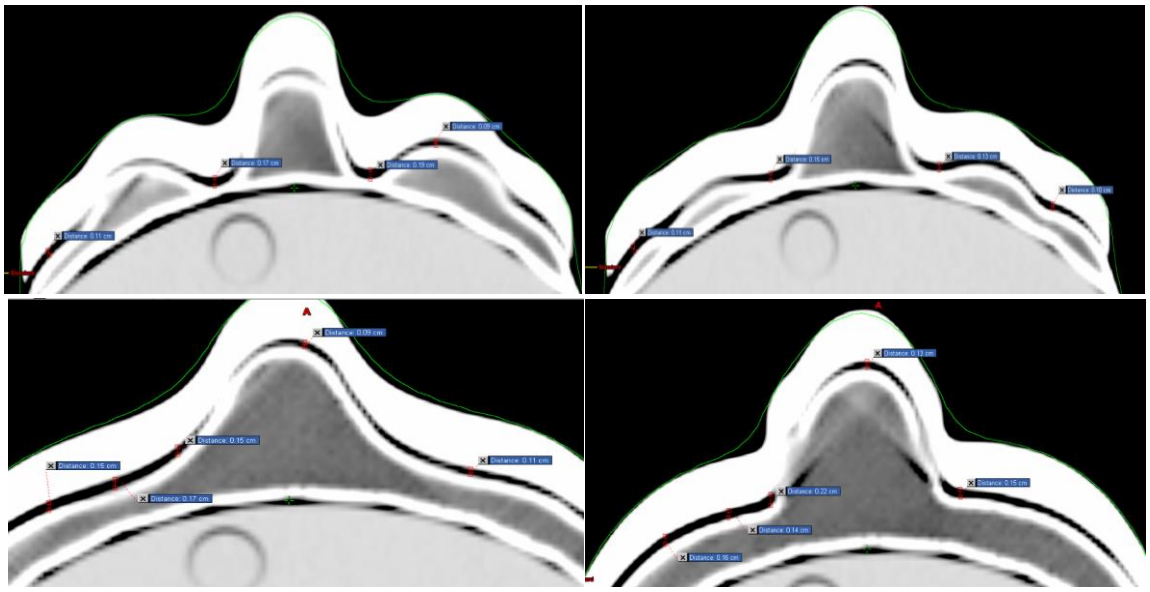

Fig 52. Air gaps formed below the 1 cm thickness 3D printed PLA bolus